

Optical Contact Lenses Biosensors

Xiaoye Xia, Yubing Hu, Nan Jiang, and Ali K. Yetisen*



Cite This: *ACS Sens.* 2025, 10, 7231–7251



Read Online

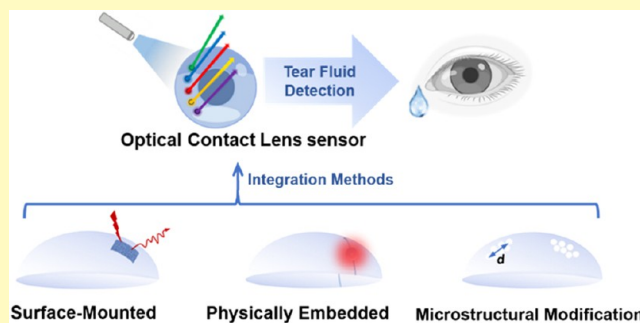
ACCESS |

Metrics & More

Article Recommendations

ABSTRACT: Tear fluid contains a diverse array of biomarkers reflective of both ocular and systemic health, making it a valuable medium for noninvasive diagnostics. Contact lens biosensors, integrated with optical sensing technologies, provide a promising platform for real-time, continuous monitoring of tear fluid composition. This review focuses on recent advances in the development of contact lens biosensors for optical detection of tear-based biomarkers. Key components include biocompatible lens materials, such as hydrogels and silicone hydrogels, that maintain oxygen permeability and optical clarity, along with fabrication methods such as inkjet printing, micropatterning, and three-dimensional (3D) microfabrication for precise sensor integration. Optical sensing mechanisms, including fluorescence, photonic crystal resonance, and surface plasmon resonance, have demonstrated high sensitivity in detecting glucose, lactate, electrolytes, cortisol, and inflammatory markers at clinically relevant concentrations. Such sensors have shown potential in diagnosing and monitoring diseases including diabetes, dry eye syndrome, stress-related disorders, and neurodegenerative conditions. Despite these advances, challenges remain in minimizing background interference, enabling long-term wear, and achieving multiplexed detection. Future research should prioritize robust biorecognition chemistries, wireless optical readouts, and scalable manufacturing strategies to support clinical translation. Contact lens biosensors are poised to become a key platform in next-generation, personalized healthcare through noninvasive tear fluid analysis.

KEYWORDS: *contact lens sensor, optical biosensing, ocular diseases, neurodegenerative diseases, microfabrication techniques*



Ocular diseases, including ametropia, glaucoma, and cataracts, significantly diminish patient quality of life and represent a major global health burden. The World Health Organization reported in 2023 that over 2.2 billion people worldwide currently live with visual impairments, at least half of which could be prevented or managed effectively with earlier and more precise diagnostic interventions.⁴ Despite rising demand for personalized healthcare driven by improved living standards, traditional diagnostic tools for ocular diseases remain episodic, invasive, and typically yield only fragmented snapshots of a patient's condition. Current clinical and point-of-care (POC) diagnostic methods, such as blood tests and ocular examinations, often suffer from limited patient compliance and inconsistent follow-up due to their invasiveness, discomfort, and inconvenience.^{6–11} Thus, there is an urgent clinical need for wearable, continuous, and noninvasive monitoring platforms that deliver real-time, accurate physiological data at the point of care, enabling earlier diagnosis, timely intervention, and truly tailored patient management.

Recent advances in flexible and stretchable substrates have catalyzed the development of conformable, wearable diagnostic platforms capable of continuous, noninvasive health monitoring.^{12–15} In parallel, breakthroughs in microelectronics have facilitated the miniaturization of sensors and onboard signal

processing, dramatically reducing the need for bulky instrumentation.^{16,17} Concurrent innovations in optical biosensing—including photonic waveguides, fluorescence-based assays, and plasmonic sensing—now offer unprecedented molecular sensitivity, specificity, and multiplexing capabilities on flexible substrates.^{18–21} Collectively, these technological advancements underpin next-generation wearable biosensors that can continuously detect metabolites, ions, proteins, and physical parameters such as temperature, pressure, and electrophysiological signals directly from biofluids.^{22–28}

Among wearable diagnostic devices, contact-lens-based sensors hold distinct advantages, given their direct access to tear fluid and proximity to the corneal surface—both rich sources of biomarkers that closely reflect ocular as well as systemic health conditions, including metabolic disorders, inflammatory diseases, and neurological impairments.^{29,30} Tear fluid is continually replenished at approximately 0.5 μ L per

Received: April 12, 2025

Revised: September 3, 2025

Accepted: September 11, 2025

Published: October 2, 2025



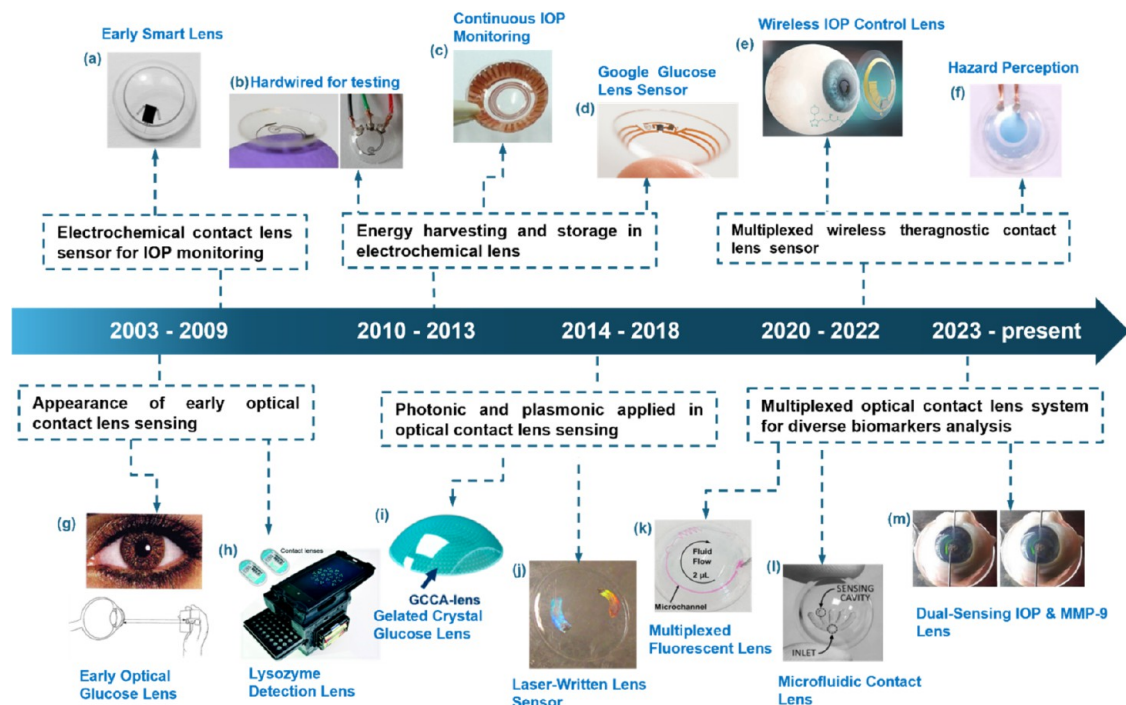


Figure 1. Timeline of contact lens sensor development. (a) Wireless contact lens sensor for intraocular pressure monitoring. Copyright 2008 Acta Ophthalmol.^{38,39} (b) Contact lens with embedded sensor for monitoring tear glucose level.⁴⁰ Copyright 2011, with permission from Elsevier. (c) A capacitive contact lens sensor is used for continuous monitoring of intraocular pressure.⁴¹ Copyright 2013, with permission from Elsevier. (d) Google's project for commercialized contact lenses for glucose sensing.⁴² Copyright 2017 American Chemical Society. (e) Wireless theragnostic contact lens for monitoring and control of IOP.⁴³ Copyright 2022 Springer Nature. (f) Contact lenses for hazard perception.⁴⁴ Copyright 2020, with permission from Elsevier. (g) Early optical glucose-sensing contact lens.⁴⁵ Copyright 2005, with permission from Elsevier. (h) Lysozyme detection in tears using a contact lens with a mobile sensor.⁴⁶ Reproduced with permission from the Royal Society of Chemistry. (i) A gelated crystal-attached lens for continuous glucose sensing.⁴⁷ Copyright 2017 MDPI. (j) Direct-laser writing of contact lens sensor.⁴⁸ Copyright 2018 American Chemical Society. (k) Multiplexed fluorescent scleral lens sensor for tear ions measurement.⁴⁹ Copyright 2019 A. K. Yetisen. Published by WILEY-VCH Verlag GmbH & Co., KGaA, Weinheim. (l) A paper-based microfluidic contact lens platform for tear pH, glucose, proteins, and nitrite ions sensing.⁵⁰ Copyright 2020, with permission from Elsevier. (m) Contact lens dual-sensing platform for monitoring IOP and matrix metalloproteinases-9 (MMP-9).⁵¹ Copyright 2022. Advanced Science published by Wiley-VCH GmbH.

minute, contains clinically relevant biomarkers in measurable concentrations, and provides a convenient, painless sampling approach suitable for patient-friendly diagnostics.^{33–36} Additionally, contact lenses are already widely adopted by more than 150 million individuals globally for vision correction and cosmetic purposes, positioning them ideally for seamless integration of sensing functionalities without significant lifestyle disruptions. Indeed, recent pioneering efforts have successfully demonstrated the feasibility of real-time tear glucose monitoring in diabetic patients, continuous tracking of inflammatory biomarkers for dry-eye disease, and around-the-clock intraocular pressure monitoring for improved glaucoma management.^{33–36}

Despite these promising advances, significant challenges persist in achieving an optimal balance between biocompatibility, sensor performance, power efficiency, and user comfort. Minimizing optical background interference from tear-fluid constituents and maintaining long-term sensor stability during extended wear are critical obstacles for clinical translation. Addressing these hurdles requires innovations in materials science, surface engineering, and signal amplification methods, as well as the establishment of robust protocols for large-scale manufacturing and standardized clinical validation.

The journey toward integrating sensing elements into contact lenses began with the invention of the poly-(hydroxyethyl methacrylate) (pHEMA) hydrogel lens by

Wichterle in 1970, transitioning the market from rigid poly(methyl methacrylate) (PMMA) lenses to more comfortable and scalable soft hydrogels.⁵² Over subsequent decades, steady advancements in lens materials—particularly regarding biocompatibility and fabrication precision—laid the groundwork for embedding biosensors directly within contact lenses (Figure 1i). Around 2010, developments in microelectromechanical systems (MEMS), flexible electronics, and micro-fabrication enabled electrochemical sensing modules, typically relying on enzymes like glucose oxidase or lactate oxidase, to be embedded in lenses.^{36,37,42,53} Although enzyme-based systems demonstrated excellent analytical sensitivity, they faced inherent limitations, such as enzyme degradation, short operational lifetimes, and frequent recalibration requirements, alongside discomfort caused by integrated electronic components and power modules.^{54,55}

Optical sensing technologies provide real-time readout, high sensitivity (often nM to pM) and straightforward multiplexing, while avoiding the enzyme instability and hard-wired electronic interfaces typical of electrochemical designs (Figure 2). Techniques such as photonic crystals,^{56,57} holographic gratings,^{58–60} Förster resonance energy transfer (FRET)-based probes,^{58,61} and surface-enhanced Raman scattering (SERS) sensors enable label-free, real-time monitoring with exceptional sensitivity and multiplexing capabilities. By detecting subtle optical changes—shifts in diffraction wave-

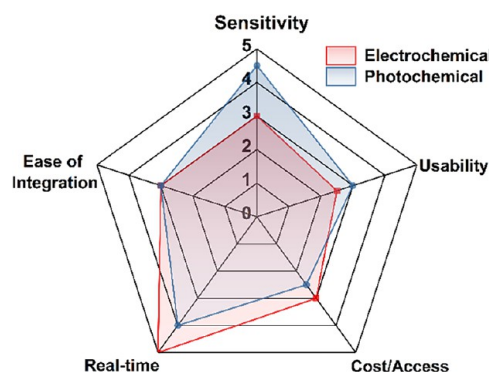


Figure 2. Electrochemical vs photochemical contact-lens sensing—trade-off summary. The radar plot shows normalized scores for sensitivity, usability, cost/accessibility, real-time feasibility, and ease of integration.^{1,2}

length, fluorescence intensity variations, or Raman scattering enhancement—these optical platforms can directly quantify low-abundance proteins, metabolites, electrolytes, and hormones within tear fluid, all without the instability issues inherent in enzyme-based methods or the complexity of wired electronic interfaces.^{62,63}

Although substantial progress has been achieved, major engineering challenges remain in seamlessly integrating these advanced optical sensors into contact lenses. Achieving reproducibility and durability without compromising comfort, vision clarity is crucial for user acceptance. Rigorous clinical testing is also necessary to ensure sensor accuracy, robustness against fluctuations in tear film, and reliability in diverse environmental conditions. Furthermore, a comprehensive review highlighting recent advances in contact lens optical sensing materials, fabrication approaches, and integration methods remains notably absent from the current literature. This review, therefore, systematically examines optical biosensor integration from substrate selection—covering rigid, soft hydrogel, and hybrid lens materials—to detailed

sensor embedding strategies within lens surfaces, intermediate layers, and internal microstructures. Lastly, we outline the path toward clinical translation, clearly delineating current technological gaps and future directions to realize contact lens-based diagnostics for real-time, point-of-care monitoring of ocular and systemic diseases.

■ TEAR FLUID-BASED BIOSENSING FOR POC DIAGNOSTICS

Alternative sample types that can replace blood in noninvasive diagnostics have been the focus of intense investigation for over a decade.^{64,65} And can potentially be used for disease screening.⁶⁶ In general, the tear film consists of an ultrathin lipid layer, a bulk aqueous layer, and an innermost mucin layer (Figure 3). The formed liquid barrier between the air and the proximal ocular tissue keeps the cornea moist and maintains the ocular antibacterial system.⁶⁷

Tear fluid has demonstrated significant value in disease diagnosis and monitoring, extending beyond ocular pathologies. In healthy eyes, the blood-tear barrier restricts the movement of compounds, such as albumin and xenobiotics, between the tear film and blood. In diseased eyes, this barrier may be compromised, leading to increased permeability, greater systemic absorption, and reduced ocular drug bioavailability due to interactions with tear proteins. Research indicates that tear fluid closely resembles the ultrafiltrate of blood plasma. Mitochondrial energy metabolism and specific metabolic processes during plasma leakage facilitate the transfer of components from the blood to tears.^{68,69}

Tear fluid's relatively simple matrix compared to serum and plasma, together with its rich reservoir of biochemical and biophysical markers (Table 1), makes it an ideal medium for point-of-care diagnostics. Ocular conditions, including keratitis and allergic conjunctivitis, are readily identified through changes in tear analytes.^{70,71} While glaucoma monitoring has leveraged matrix metalloproteinases (MMPs) and their tissue inhibitors (TIMPs).⁷⁰ Electrolyte profiles (K^+ , Na^+ , Ca^{2+}) distinguish dry-eye subtypes such as lacrimal gland dysfunction

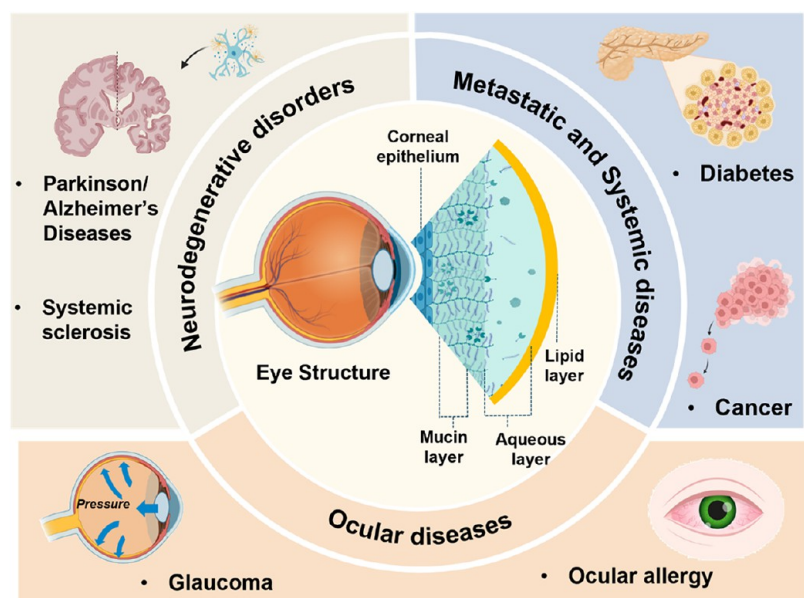


Figure 3. Tear fluid based biosensing for POC diagnostics. Schematic representation of the eye, tear layers, and four diagnostic categories (Neurological, Metastatic, Ocular, Systemic).

Table 1. Summary Table of Representative Tear Biomarkers, Associated Conditions, and Typical Concentration Ranges

category	biomarker	disease/condition	typical tear concentration	ref
neurological	α -antichymotrypsin	multiple sclerosis	~1.2–2.3 μ g/mL	3
	TNF- α	diabetic retinopathy (NPDR \rightarrow PDR)	1.2–5.5 pg/mL (NPDR); up to 21.7 pg/mL (PDR)	5
metastatic	lacryglobin	breast and other cancers	detected in 60–100% patients	31
	sulf-1; AMPK γ 3	cancer metastasis (proteomic study)	qualitatively detected (n.d.)	32
ocular	lysozyme C	general ocular surface health	~1.4 mg/mL	32
	lactotransferrin	dry eye syndrome	~1.0 mg/mL	32

Table 2. Comparison between Different Categories of Contact Lens Materials

	material	comfort	DK value (Barr)	EWC (%)	lens thickness	durability
hard lenses	PMMA	initially less comfortable, longer adaptation period	8–10	N/A	0.12–0.20 mm	2–3 years
	RGP		>30	N/A		
soft silicon lenses	SIMA	relatively comfortable, high oxygen permeability; low tolerance	10–30	38–70	0.07–0.1 mm	one day to half a year
	SIA					
soft hydrogel lenses	TRIS					
	HEMA	require short period for adaptation; short wearing period	60–150	30–60		
	PVA					
hybrid lenses	MAA					
	rigid center (RGP) with soft outer skirt (SiHG)	combines clear vision with comfort but costly	central: 10–60 peripheral: 60–160	50 for SiHG part	~0.2 mm	depends on the hybrid materials

(LGD) and meibomian gland dysfunction (MGD).⁴⁹ Beyond ocular pathologies, systemic disorders are reflected in tear fluid: elevated glucose signals diabetes,⁷² increased lacryglobin correlates with cancer metastasis,^{72,31} and detectable TNF- α marks Parkinson's disease.^{73,74} Complementary metrics—tear volume, moisture content, and intraocular pressure (IOP)—provide additional insight into ocular health.^{75,76}

Over the past decade, optical contact-lens biosensors have harnessed these tear biomarkers using fluorescence,^{7,55,67,68} colorimetric,^{77–80} and photonic-crystal^{47,48} platforms. They were fabricated focused on both paper- and lens-based substrates. These innovations have expanded the detectable panel and pushed detection limits into the low micromolar and nanomolar ranges, yet achieving high selectivity for low-abundance analytes while minimizing background interference remains a critical challenge.⁸¹ Future work must refine sensor chemistries and integration strategies to fully realize the promise of tear-based POC diagnostics.

CONTACT LENS MATERIALS

Contact lens sensors represent a significant advancement in wearable technology, merging the fields of optics and material science to enhance vision and health monitoring. These sensors are embedded into contact lenses using advanced materials tailored for specific properties. Typically, they employ flexible, ultrathin substrate materials that conform to ocular curvature, ensuring comfort and functionality. Additionally, the water content of the materials significantly impacts comfort, while mechanical properties influence durability and resistance to deformation during handling. Optical properties, including transparency and refractive index, are vital for effective vision correction. For medical applications, these lenses must also meet stringent regulatory standards while addressing the end wearer's priorities for comfort, durability, and ease of use.^{52,82} The integration of biosensing capabilities further exemplifies how materials science should advance the functionality and versatility of contact lens sensors for noninvasive health monitoring and personalized medical care.⁸³

Polymeric materials are widely used in the development of contact lens sensors, primarily due to their capacity for postfunctionalization that enhances sensing performance. These materials are crucial for integrating sensing technologies, enabling real-time monitoring of

ocular conditions and the detection of tear biomarkers. Commonly used polymers in such applications include hydrogels and specialized polymers, chosen for their good biocompatibility and mechanical stability.^{84–87} In addition, these polymeric materials provide a structural matrix for drug delivery. This dual functionality supports not only biosensing but also the controlled release of drugs directly to the ocular surfaces, thereby maximizing therapeutic efficacy. These materials can also act as a protective barrier to shield the ocular surface from harmful substances while maintaining specific properties, such as oxygen and liquid permeability.

Proper lens curvature and thickness are essential to minimize irritating tear production and avoid localized inflammation.⁸⁸ The microfabrication of sensing material always results in a shift of structural strength. A tensile strength of 0.3–1.5 MPa ensures contact lenses withstand mechanical stresses from insertion, removal, and blinking without permanent deformation. It is also essential to maintain a comfortable, nonirritating interface for adequate and consistent optical performance throughout daily wear.⁸⁹ Current commercialized contact lenses can be divided into three main categories by softness: hard lenses, hybrid contact lenses, and soft contact lenses (Table 2). Although rigid contact lenses are less comfortable, their specific functions in correcting certain corneal irregularities, such as irregular corneal astigmatism and its associated diseases, cannot be ignored. Despite this, soft contact lenses are expected to dominate the commercial market due to their superior comfort and convenience for daily use.

Hard Lenses. The most widely used rigid contact lens material, as a substitute for traditional glass material, is PMMA, which was selected for its advantages of lightweight and durability.^{90–92} The intermolecular forces, including dipole–dipole interactions and mechanical interlocking inside the polymer structure, also led to superior rigidity. In addition, the weak mobility of the chains restricts the diffusion of water and oxygen, and prolonged wear may trigger corneal hypoxia.⁹³ A market share of less than 1% proves the inappropriateness of lens materials.⁹⁴ As an improvement, silicone acrylates were introduced in PMMA as rigid gas permeable (RGP) material to increase wearing comfort while retaining the inherent advantages of PMMA.

Soft Lenses: Pros and Cons of Hydrogel vs Silicone Hydrogel. Soft contact lenses are made of hydrogels with high water content, which gives them exceptional flexibility. Cross-linking agents, such as ethylene glycol dimethacrylate (EGDMA), can enhance its mechanical properties and gelling, thereby maintaining

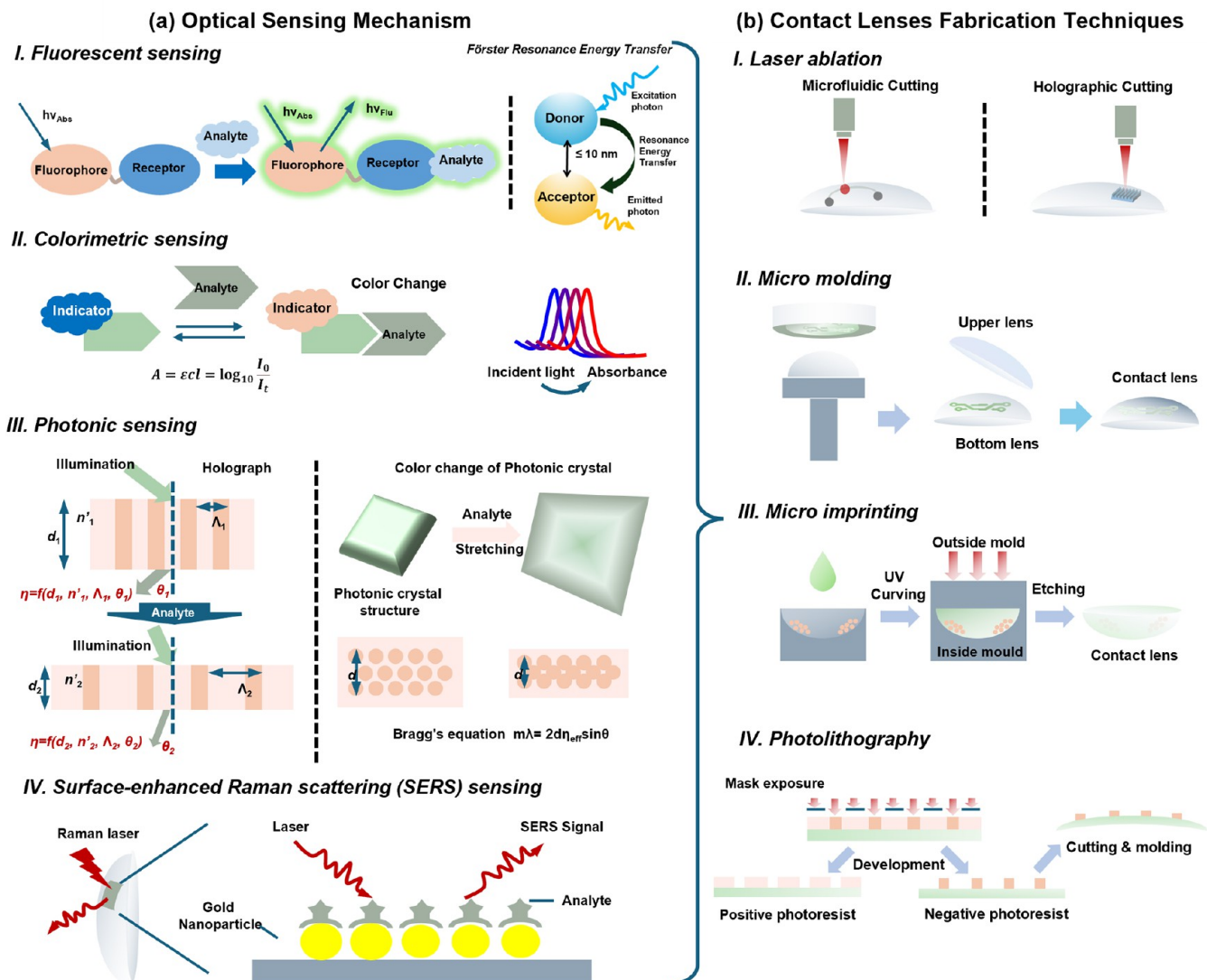


Figure 4. Assembly principle of a contact lens sensor. (a) Schematic of main optical sensing mechanisms: I. Fluorescence sensing, II. Colorimetric sensing, III. Photonic sensing and IV. SERS sensing in optical contact lens sensors. (b) Fabrication techniques to integrate the sensor in contact lens substrate materials including I. Laser ablation, II. Micro molding, III. Micro Imprinting and IV. Photolithographic.

a balance between structural integrity and oxygen permeability. As a result, they dominate the commercial contact lenses market due to their superior comfort and convenience in daily use. The two main soft lens materials include conventional hydrogels and soft silicone hydrogels.

Conventional Hydrogels. Hydrogel, including poly(vinyl alcohol) (PVA) and poly(2-hydroxyethyl methacrylate) (pHEMA), has a broad market application prospect. PVA is a relatively new synthetic polymer that offers the advantages of high biocompatibility and hydrophilicity due to the presence of a hydroxy group in its monomer, resulting in high tensile strength and low protein absorption for contact lenses. However, its low gas permeability, similar to that of PMMA, requires improvements for long-term comfort and eye health. Hydroxyethyl methacrylate (HEMA) is another popular material for commercial application; it is commonly copolymerized with monomers (e.g., Methacrylic Acid or *N*-Vinyl-2-pyrrolidone) to create pHEMA hydrogels, improving wettability and structural stability.^{95,96} Despite some incompatibilities with microfabrication technologies, pHEMA's excellent transparency and mechanical properties make it ideal for advanced diagnostic and therapeutic contact lens applications.

Silicone Hydrogels. Contact lenses made of silicone hydrogel have already occupied the most significant contact lens market share due to

their durability for long-term use, coming from the intrinsic and robust silicon–oxygen bonding.^{97,98} However, the lenses' inherent hydrophobicity reduces their biocompatibility. For biosensing applications, Badugu et al. discovered that silicone hydrogel lenses have regions that interact with water-soluble molecules and hydrophobic zones that bind nonpolar molecules. These properties have been utilized in designing biosensors to detect various elements.^{99–101}

Hybrid Lenses. The hybrid lenses are primarily designed to have a central zone made of RGP materials with high optical properties and a peripheral zone made of silicone hydrogel, which is more comfortable to wear. The overall larger diameter of the hybrid lenses also brings the tendency toward the center. Moreover, problems exist, such as a tight fit in the peripheral segment and deposit formation.^{9,10} Breakage at the RGP/hydrogel junction was also reported to be as high as 48.5% of cases fitted with SoftPerm lenses.⁶ The optimized lens materials could not only deliver both comfort and clear vision but also define discrete regions for biosensor integration.

Table 3. Comparative Performance of Optical Sensing Modalities for Tear-Fluid Biosensing

modality	LOD	specificity	ease of Integration	clinical/field validation	ref(s)
fluorescence	glucose: 0.01 mM; Na^+ : 120 mM	high	moderate (requires optics)	human diabetic trial: tear-glucose lens readout <1 min, $R^2 = 0.92$ vs blood glucose in 8 volunteers	109, 110
colorimetric	lactate: 0.03 mM; pH: ± 0.1 unit	moderate	easy (embedded reagent)	sweat-chloride patch for cystic fibrosis: $\geq 98\%$ sensitivity, at 60 mM cutoff	111, 112
photonic	sweat glucose: 0.12 mM	high	challenging (microfabrication)	wrist-watch SPR sensor, $R^2 = 0.95$ vs blood glucose in $n = 10$ human subjects	113, 114
SERS	SARS-CoV-2 N-protein: 5.2 PFU/mL	very high	difficult (nanostructure)	SERS-LFIA assay: rapid COVID-19 antigen test vs RT-PCR ($n = 60$ samples)	108

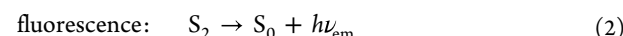
■ PRINCIPLES OF OPTICAL SENSING IN CONTACT LENS

One of the key advantages of optical contact lens sensors is their ability to incorporate a range of sensing techniques enabled by a range of fabrication methods (Figure 4). Fabrication technologies, such as laser ablation, micromolding, microimprinting, and photolithography, allow for the precise integration of sensors within the lens architecture during contact lens production. By creating microfluidic channels inside the lens via micro molding or a laser ablation, changes in signals within specific areas can be more precisely localized and captured by portable readout devices.^{50,102,103} Additionally, microimprinting or direct modifications integrate fluorescence, colorimetric probes, or crystalline colloidal arrays (CCA) inside the substrate materials, providing overall signal variations and balance signal detection capabilities with minimal alterations to the material properties of the lenses.^{76,104}

As summarized in Table 3, each optical sensing modality offers distinct advantages and disadvantages specifically relevant to contact lens integration. Fluorescence-based lenses have demonstrated successful real-time glucose monitoring in diabetic patients, combining high sensitivity and rapid response, although the embedded optics can present integration challenges and potential discomfort.¹⁰⁵ In contrast, colorimetric contact lens sensors provide simplicity and optics-free operation, making them user-friendly, though they sacrifice sensitivity and real-time capabilities.^{76,106} Photonic sensors enable multiplexed, label-free detection with high specificity but require complex microfabrication, increasing manufacturing difficulty and cost.^{60,107} Finally, SERS-based lenses have achieved ultrasensitive, low-abundance biomarker detection (down to picomolar levels), offering immense diagnostic potential, yet their implementation is hindered by complex nanostructured substrates and higher production costs.¹⁰⁸ These examples collectively confirm the feasibility and versatility of integrating optical sensing modalities into contact lens platforms, each with trade-offs in sensitivity, complexity, cost, and real-world applicability. Consequently, essential health data is provided seamlessly without disrupting daily activities. Each optical modality has been validated beyond the bench, from diabetic-volunteer pilots and approved diagnostic assays to human wearables and clinical specimen tests. These confirm both their readiness for in vivo use and the feasibility of integrating them into contact-lens sensor platforms.

Fluorescence Sensing. Fluorescence biosensors have become increasingly important due to their high sensitivity, specificity, ease of use, and relatively low cost.^{115–117} It readily reach nM– μM LODs for glucose and ions, making them ideal for metabolic monitoring in tears,^{35,49} with performance dependent on factors such as sensor status, detection range, and response time. Key principles for strong fluorescence

include absorption at wavelengths that prevent molecular dissociation and a faster rate of radiation than intramolecular energy transfer. Advanced technologies, such as FRET, enable multianalyte monitoring within a single detection system, improving diagnostic accuracy for ocular diseases and enhancing clinical studies. FRET occurs when an excited donor fluorophore transfers energy to a nearby acceptor, resulting in decreased donor fluorescence intensity and lifetime while increasing acceptor emission. Unlike direct fluorescence detection, FRET remains unaffected by fluorophore concentration fluctuations, reducing interference from photobleaching and diffusion. Its ability to minimize light scattering enhances the accuracy of in vivo sensing. Moreover, fluorescence is highly molecule-specific as it depends on the chemical composition of the target fluorophore. This specificity makes FRET particularly effective for detecting tear biomarkers associated with conditions such as dry eye disease and diabetic retinopathy.



Fluorescence in contact lens sensors has raised attention to their specificity and versatility. For example, with the advantages of assessing the severity of dry eye disease and differentiating its subtypes, studies have been performed to develop fluorescent contact lens sensors to monitor physiological levels of pH, Na^+ , K^+ , Ca^{2+} , Mg^{2+} , and Zn^{2+} ions, providing quantitative data via smartphone readouts.^{99,118,119} The continuous evolution of fluorescence sensing technologies holds significant promise for real-time ocular disease diagnosis and understanding of ocular physiology.

Colorimetric Sensing. Colorimetric sensing leverages enzymatic reactions to achieve μM – mM detection ranges with high specificity. It is simple, reagent-based format can be readily implemented on paper- or lens-embedded platforms.^{120,121} Most of colorimetric contact lens sensors functioned based on the Beer–Lambert law, $A = \epsilon cl = \log_{10} \frac{I_0}{I_t}$. In which A is the absorbance, ϵ represents molar absorptivity or the extinction coefficient, c is the concentration in the tear liquids, and l represents the path length of the sample, while I_0 and I_t are the intensity of incident and transmitted light separately. It quantitatively helps for the derivation of the concentration change in solution by measuring the absorbance of the incident light, accompanied by visible color change, which could also be specified and calculated in an RGB graph.

Riaz et al. proposed a dynamic ocular pH biosensor utilizing anthocyanins, which change chemical structure and color at different pH levels.⁷⁸ Extracted from *Brassica oleracea*, anthocyanins were used to functionalize commercial soft contact lenses through soaking and drop-casting processes,

with an optimized soaking time of 24 h. The sensors exhibited negligible dye leakage over 18 h and demonstrated a correlation between pH and color (measured via RGB triplets), indicating potential for continuous POC applications.⁷⁸

Photonic Sensing. Photonic crystals (PCs) are composed of periodically ordered materials with varying refractive indexes based on the direction of periodicity and are classified into one- to three-dimensional (1–3D) structures. When illuminated by polychromatic light, these crystals diffract light according to Bragg's law. Accordingly, the diffracted wavelength changes due to any modification in the periodic constant or the effective refractive index. Subnanometer changes in lattice spacing or refractive index yield a pronounced diffraction-peak shift. Alexeev et al. demonstrated a detection limit of $\approx 1 \mu\text{M}$ glucose in synthetic tear fluid, with diffraction peaks shifting by 10 nm over a 0.1–0.6 mM glucose range.¹²²

Photonic sensors have been integrated into contact lenses as forms of holographic gratings or CCA.^{47,122–127} Generally, 1D photonic structures are fabricated utilizing deposition or laser ablation, while 2D and 3D structures are obtained by photolithography or microimprinting.^{59,60,128,129} The diffraction of light derived from structural change indicates minimal alteration on the PC plane, allowing for the quantification of tear analytes through color variations. Multiple studies have developed contact lens sensors with holographic gratings to test glucose in tear fluid at various physiological pH conditions and ionic strengths.^{130,131}

3D photonic crystal array sensors are particularly notable, comprising nanosized particles immobilized within polymer matrices. These arrays are formed from crystalline nanospheres, such as polystyrene and silica, that self-assemble into ordered structures upon the evaporation of colloidal solutions. The photonic CCA-based sensors are embedded within a polymer matrix that diffracts light in the visible spectrum. Such advanced PCs have been widely investigated for tear-based diagnostics, offering precise and responsive sensing capabilities. The dye-free nature of photonic sensors avoids the use of dyes and keeps them away from photobleaching, resulting in a longer use time.

Surface-Enhanced Raman Scattering (SERS) Sensing. Surface-enhanced Raman scattering (SERS) amplifies intrinsically weak Raman signals at plasmonic "hot spots" formed near nanostructured Au/Ag features, providing label-free molecular fingerprints with ultrahigh sensitivity (down to the pM regime) and rapid spectral readout.^{132,133} On contact lenses, SERS elements are typically introduced by surface transfer/stamping of prepatterned metallic films or by *in situ* immobilization of nanoparticles, nanoislands, or nanobowls within the hydrogel matrix. These strategies localize intense electromagnetic fields at the tear–lens interface, enabling detection of low-abundance biomarkers under physiologically relevant conditions. Using such architectures, proof-of-concept lenses have quantified glucose with high sensitivity, and related platforms have reported SERS readout of proteases/cytokines at clinically meaningful concentrations.^{78,134–136}

Design considerations strongly influence performance and safety. Plasmonic resonance tuning (particle size/shape, intergap spacing, lattice periodicity) is matched to NIR excitation to reduce hydrogel autofluorescence and ocular absorption, while thin dielectric shells and PEG/zwitterionic coatings mitigate ion leaching, nonspecific adsorption, and

biofouling in the protein- and salt-rich tear film.^{137–139} Stable anchoring chemistries, including thiol–Au, catechol–metal, UV-cross-linked interpenetrating networks, prevent nanoparticle migration during wear, and peripheral or annular SERS zones help preserve pupil optics and wearer comfort. From a manufacturing standpoint, SERS features must remain compatible with sterilization (UV/EtO/ γ) and saline storage without loss of enhancement, while maintaining hydrogel transparency and modulus.^{140–142}

■ OPTICAL READOUT AND MITIGATING INTERFERENCE OF CONTACT LENS SENSOR

Readout options for contact-lens sensors include fluorescence, colorimetric, photonic/holographic, and SERS, each with practical constraints: fluorescence and SERS are reliable with brief *ex vivo* interrogation; colorimetry supports low-cost and fast imaging; photonic/holographic diffraction remains alignment-sensitive.

Smartphone Integration in Fluorescence Readout. Signals from fluorescence-based contact lens sensors are typically captured using either compact benchtop fluorimeters or smartphone cameras combined with a custom-designed, 3D-printed lens holder. In most current setups, lenses are briefly removed (< 1 min) and placed within holder, where they are illuminated by a low-power LED with an appropriate excitation wavelength.^{62,143} An integrated optical filter positioned between the lens and detector isolates the fluorescence emission, reducing background interference and enhancing signal clarity. The emitted light is captured by the smartphone camera or a small photodiode detector, and the resulting signal is analyzed by dedicated software or smartphone apps to quantify biomarker concentration. However, this approach introduces additional complexity, increased power demands, and higher costs, requiring careful optimization to ensure practical usability and comfort.

RGB Imaging for On-Lens Assays in Colorimetric Readout. Color changes in colorimetric contact lens sensors can be read by eye for semiquantitative use or precisely quantified using smartphone apps that analyze RGB values. Because no external optics are required, users can remove the lens for a 10 s photo, making this the cheapest and most accessible modality.^{144,145}

Holographic Readout: Alignment-Sensitive Readout. Reading out of photonic-based lenses currently relies on external spectrometers or smartphone attachments, as precise optical alignment and careful calibration remain challenging. While proof-of-concept goggles integrating on-eye readout optics have been demonstrated experimentally, practical limitations in alignment precision, complexity, and cost have largely confined photonic sensors to clinical or research environments rather than routine home use.^{60,146,147}

SERS Readout: Practical Constraints. Current implementations rely mainly on brief *ex vivo* interrogation: the lens is removed and placed in a holder on a benchtop Raman system to ensure stable excitation, precise alignment, and high detector sensitivity.^{132–134} Signal processing, including baseline correction and drift compensation, can further enhance specificity in the presence of eye motion and tear-film fluctuations.^{148,149} At present, SERS contact lenses are suited to high-sensitivity spot assays and clinical tear-specimen testing; continuous on-eye monitoring remains a future objective depending on stability and motion-robust quantitative spectroscopy.

Table 4. Principal and Performances of Contact Lens Sensors

sensing mechanism	lens materials	analytes	bioactive molecule	detection range	limit of detection	response time	ref(s)
fluorescence	PVA pHEMA	glucose Na ⁺ K ⁺	boronic acid containing fluorophores (BAFs) diaza-15-crown-5 (DA15C5) diaza-15-crown-5 (DA18C6)	50–500 μ M 0–100 mM 0–50 mM	15.6 mM 8.1 mM	— —	105 118
	Ca ²⁺ Mg ²⁺ Zn ²⁺		1,2 bis(o-aminophenoxy) ethane-N,N',N',N'-tetraacetic acid (BAPTA) 5-oxazolecarboxylic acid (SOACA)	0.5–1.25 mM 0.5–0.8 mM 10–20 μ M	0.02–0.05 mM 0.10–0.44 mM 10–20 μ M	— —	— —
	H ⁺		luorescent N-(2-methoxyphenyl) iminodiacetate (MPIDA) benzenedicarboxylic acid (BDDCA)	pH 7–8	pH 0.12	— —	— —
	SiHG	Na ⁺	sodium green	—	0.3 mM	—	119
	SiHG	Cl ⁻	SPQ-C18	—	10 mM	—	99
	H ⁺		6HQ-C18	—	pH 6.5–7.0	— —	— —
	Nafilcon A	glucose	NBD-C18	— —	— —	— —	155, 156
	SiHG	glucose	tetramine isothiocyanate–concanavalin A (Tritic_Con A)	— —	<100 mM 9.3 μ M	— 3–5 s	100 157
	pHEMA	glucose	Qin-C18	— —	— 0.1 mM	— —	— —
	pHEMA	glucose	GS-NHS	— 0.1–1 mM	0.1 mM 0.23–0.8 mM	— 10–13 s	— 63
	SiHG	ascorbic acid	cerium oxide nanoparticles	— 0.23–0.8 mM	0.23 mM	— —	— 62
	SiHG	lactoferrin	bovine serum albumin (BSA-AuNCS)	— 0.44–5 mg mL ⁻¹	0.44 mg mL ⁻¹	— —	— —
	SiHG	lysozyme	trivalent terbium (TbCl ³)	— —	1.99 μ g mL ⁻¹	10 min	46
	pHEMA	glucose	<i>Micrococcus lysodektilicus</i>	— 3,3',5,5'-tetramethylbenzidine (TMB)	1.1–10.0 mM 1.1–8.0 mg mL ⁻¹	1.1 mM 1.1 mg mL ⁻¹	15 s 106
	pHEMA	protein	3',3'',5,5''-tetrachlorophenol-3,4,5,6-tetra bromsulphophthalein	— —	0.059–1.0 g L ⁻¹	0.059 g L ⁻¹	15 s
		L-ascorbic acid	phosphomolybdc acid	— —	19.2–160 μ M	19.2 μ M	25 s
		nitrite	sulfanilamide	— —	<0.11 mM	<0.11 mM	20 s
	pHEMA RGP	glucose	cerium oxide nanoparticle–poly(ethylene glycol) glucose oxidase (COP)	29–40 °C	— —	10 min 490 ms	104 159
		corneal temperature	cholesteryl oleyl carbonate (COC), cholesteryl nonanoate (CN), and cholesteryl benzoate (CB)	— —	— 2.14 μ g mL ⁻¹	— 2.14 μ g mL ⁻¹	— 34
			CD81 antibodies	— —	1–4 kPa 33–38 °C	0.18 kPa —	160 76
	pHEMA	exosome	chromogenic material	— —	— —	— 12 h	— 161
	pHEMA	corneal temperature	— —	— —	— 10 μ M	— —	122
	pHEMA	IOP	— —	— —	— 0.05 mM	— —	47
	pHEMA	timolol	— —	— —	— 0.006 mM	— —	123
	pCCA	glucose	4-acetamido-3-fluorophenylboronic acid diols and borate ions	— —	— —	— —	60
	GCCA	glucose	phenylboronic acid	— —	— —	— —	128
	NIR-PCCA	glucose	phenylboronic acid	— —	— —	— —	107
	PCCA	DSP	phenylboronic acid	— —	— —	— —	162
	PVA	glucose	phenylboronic acid	— —	— —	— —	163
	PDMS	glucose	4-mercaptophenyl boronic acid (MPBA)	— 500 nM–1 mM	0–50 mM 211 nM	<30 min —	— —
	SERS-LM	glucose	parylene-C	— —	— —	— —	— —
	scleral lens	protein	SERS	— —	— —	— —	— —
	pHEMA	metabolic	— —	— —	— —	— —	136

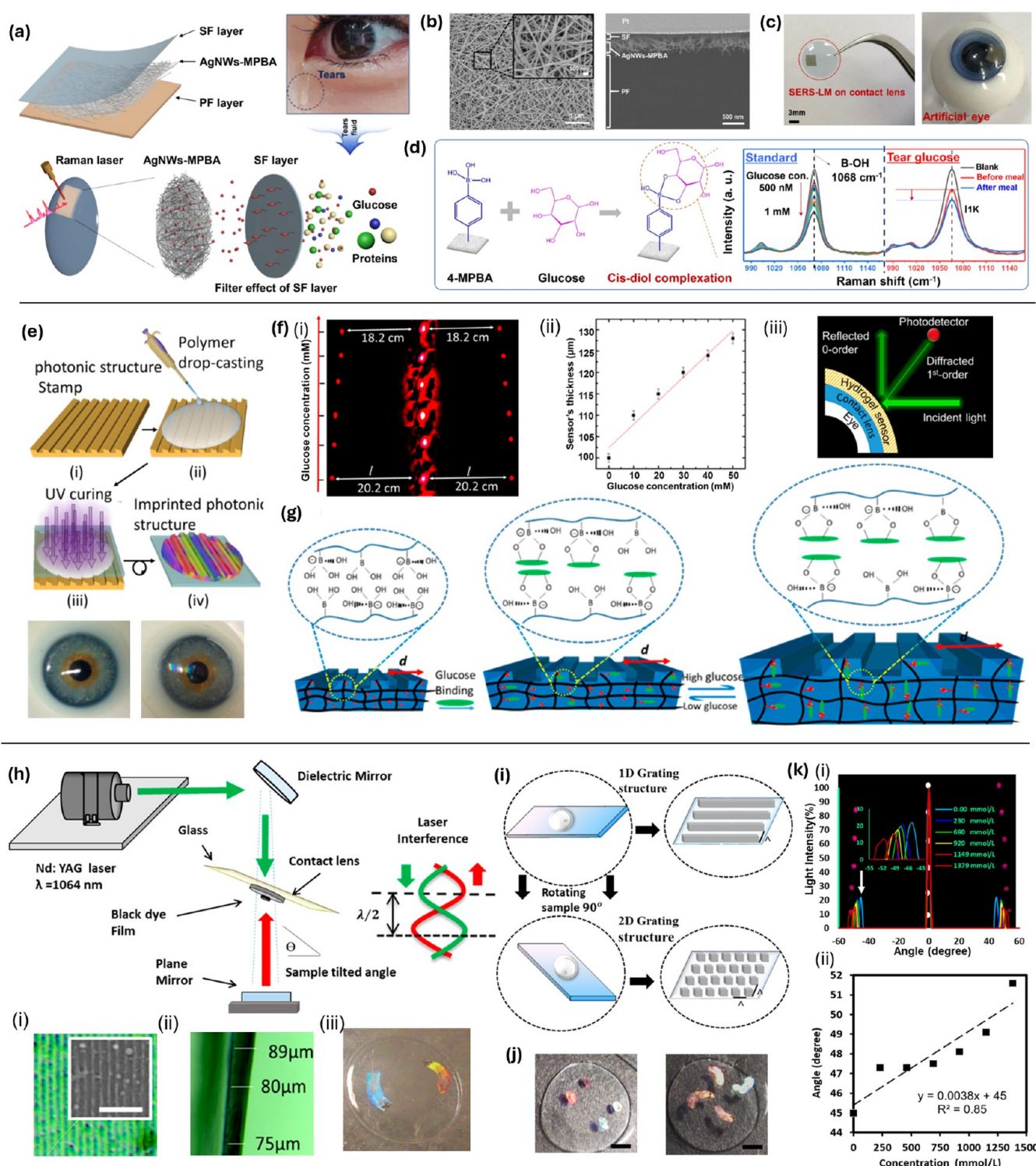


Figure 5. Surface-mounted optical sensors integrated onto the surface of contact lenses. (a) A combined SERS-LM structure integrated with a contact lens for selective glucose detection. (b) FE-SEM images show AgNWs on the SF layer, inset high-resolution nanowires, and SERS-LM cross-section after FIB cutting. (c) A prototype of the SERS-LM integrated into a contact lens. (d) The chemical selectivity of 4-MPBA for glucose with Raman spectra changes of the SERS-LM after reacting with varying glucose concentrations.¹⁶² Copyright 2020, with permission from Elsevier. (e) The fabrication of a hydrogel glucose sensor: I. A PS master is used as a stamp. II. PS is coated with monomer solution via drop-casting. III. UV polymerized monomer on contact lens. (f) i. Transmitted diffraction patterns of the PS sensor at low glucose concentrations are depicted. ii. The sensor's cross-section changes versus glucose concentration. iii. The setup for projecting diffraction patterns and measurement. (g) Glucose-phenylboronic acid complexation in the 1D PS sensor.⁶⁰ Copyright 2018 American Chemical Society. (h) One-dimensional nanopatterns on contact lenses are fabricated via DLIP with Nd laser (1064 nm, 3.5 ns). i. Optical microscopy of the 1D nanostructure with SEM (scale bar = 5 μ m). ii. Lens cross-section in ambient humidity (scale bar = 100 μ m). iii. Ink-based holographic nanostructures on lenses (scale bar = 5 mm). (i) 1D and 2D nanostructures are presented. (j) Holographic nanostructure designs (rings/patches) on contact lenses. (k) i. Diffraction measurements (ii) Calibration plot of angle (degree) versus concentration (mmol/L) with a linear fit: $y = 0.0038x + 45$, $R^2 = 0.85$.

Figure 5. continued

on nanopatterned lenses at different Na^+ concentrations. ii. Diffraction angle variations corresponding to Na^+ concentration changes.⁴⁸ Copyright 2018 American Chemical Society.

Practical Multiplexing and Interference Management. For multianalyte operation in tears, optical contact-lens sensors limit spectral crosstalk and matrix effects by selecting probe sets with well-separated excitation and emission bands. It uses ratiometric or inner-reference calibration to suppress illumination and thickness drift, partitioning chemistries into discrete microdomains or microfluidic reservoirs to prevent cross-diffusion. Image-based chemometric analysis can be applied to unmix residual overlap. Selective receptor design further enhances specificity; tetrahedral boronated receptors for glucose minimize lactate interference and mitigate pH dependence across the tear range.^{77,99,150,151}

In fluorescence sensing, dual-dye ratiometric schemes on silicone-hydrogel lenses have enabled concurrent readouts of pH, chloride, and sodium, while maintaining robustness to illumination fluctuations and thickness nonuniformity.^{99,152} In photonic and holographic designs, glucose-responsive systems using tetrahedral boronate receptors show attenuated lactate cross-reactivity and moderated pH response, and the use of a fixed reference band allows relative wavelength-shift calibration under tear-like conditions.^{29,77,153} In colorimetric microfluidics, segregated reaction reservoirs with smartphone-based RGB quantification physically isolate assays and limit diffusion crosstalk, enabling clean multiplexed measurements on-lens.⁷⁷ In SERS platforms, the intrinsic narrowness of Raman bands provides naturally separable channels for multiple targets, though stable baselines, background suppression, and reliable spot alignment remain essential; most current demonstrations therefore perform a brief *ex vivo* readout after lens removal to ensure excitation stability and detector sensitivity.^{51,154}

■ INTEGRATION OF CONTACT LENS SENSORS

As an ideal platform for precise monitoring of biomarkers in tear fluid, contact lens sensors are required to ensure effective lens-ocular surface interaction and tear collection. The sensing techniques utilized, accompanied by the choice of substrate materials and constructions, have a significant effect on the sensors' detection range and response time, with representative studies in recent years summarized in Table 4.

Surface-Mounted Optical Sensors on Contact Lens. Surface mounting uses coating or ablation to apply sensors directly, allowing postproduction modifications. The characteristic of direct contact with tear fluid also improves rapid analyte detection. Despite these benefits, sensors fabricated on the lens surface may be more vulnerable to mechanical abrasion or detachment during wear. The challenge lies in ensuring that the surface-adhered sensors remain stable and functional throughout the lens' lifespan while maintaining the necessary biocompatibility and comfort for the wearer.

Dip-Coat or Spray-Coat Plasmonic/Holographic Nano-films. Surface mounting attaches sensor films or patterns directly onto the lens exterior, offering straightforward fabrication and immediate tear contact. A contact lens sensor was developed by the fabrication of a plasmonic material prepared to transform glucose monitoring.¹⁶² This innovation utilized a layer-by-layer structure, beginning with a biocompat-

ible silk fibroin (SF) layer that doubles as a molecular filter for the screening of the protein-rich milieu of human tears (Figure 5a,b). FE-SEM and FIB cross sections confirm AgNWs on the SF layer and the layered SERS-LM architecture. Atop this selective barrier lies a layer of silver nanowires (AgNWs), which was functionalized with 4-mercaptophenylboronic acid (MPBA) to form a dense matrix of hotspots for signal amplification. These hotspots, essential for enhancing Raman signals, are meticulously arranged, as revealed by FE-SEM images, thus providing a real-time window into the wearer's glycemic state. The device's precision stems from the cis-diol complexation between MPBA and glucose, where a protective film further protects the reaction from environmental interference.¹⁶² With a detection limit of 211 nM, this multilayer SERS-LM exhibits high sensitivity; the lens-mounted prototype (Figure 5c) and concentration-dependent Raman responses consistent with 4-MPBA glucose selectivity (Figure 5d) support its potential for tear-glucose monitoring and integration into wearable biofluid-sensing systems. Another smart contact lens tailored for the continuous monitoring of glucose in real-time physiological settings was proposed by Elsherif et al. (Figure 5e–g). This innovative glucose sensor integrates 3-(acrylamide) phenyl boronic acid (3-APB) within a polyacrylamide hydrogel matrix to form a highly responsive hydrogel.⁶⁰ By employing replica molding, a 1D grating, acting as a diffraction element, was precisely engineered onto the hydrogel, which is ultimately attached to the surface of the commercial contact lens. Fabrication uses a polystyrene (PS) master as a stamp; monomer is drop-cast and UV-polymerized on the lens to form the imprinted photonic structure. This 1D grating acts as the optical transducer, converting hydrogel volumetric changes into discernible diffraction signals. Incorporation of the grating increases the sensor's surface-to-volume ratio and hydrophobicity, enabling rapid response (~3 s) and saturation (~4 min) under continuous monitoring. The device was seamlessly integrated onto a commercial contact lens for tear-glucose detection, with a smartphone's ambient light sensor used for readout. Consistent with this design, Figure 5f shows transmitted diffraction patterns at low glucose, cross-sectional changes versus glucose, and the projection/measurement setup, while Figure 5g illustrates glucose–phenylboronic-acid complexation in the 1D sensor.

Laser Direct-Write of Holographic Gratings. Another innovation in surface integration was achieved by directly writing nanophotonic structures onto contact lenses using laser technology. They deliver dye-free, real-time color shifts but require precision alignment and robust adhesion to the curved lens surface. In this study, 1D and 2D nanostructures were inscribed onto hydrogel contact lenses by employing a precisely controlled neodymium-doped yttrium aluminum garnet (Nd: YAG) laser beam to etch detailed grating structures into the lens material (Figure 5h–k).⁴⁸ One-dimensional nanopatterns were fabricated by DLIP with an Nd laser (1064 nm, 3.5 ns), with optical microscopy/SEM of the nanostructure and a lens cross-section in ambient humidity. The precision of these nanostructures was measured using SEM images. The adaptability of this method is further

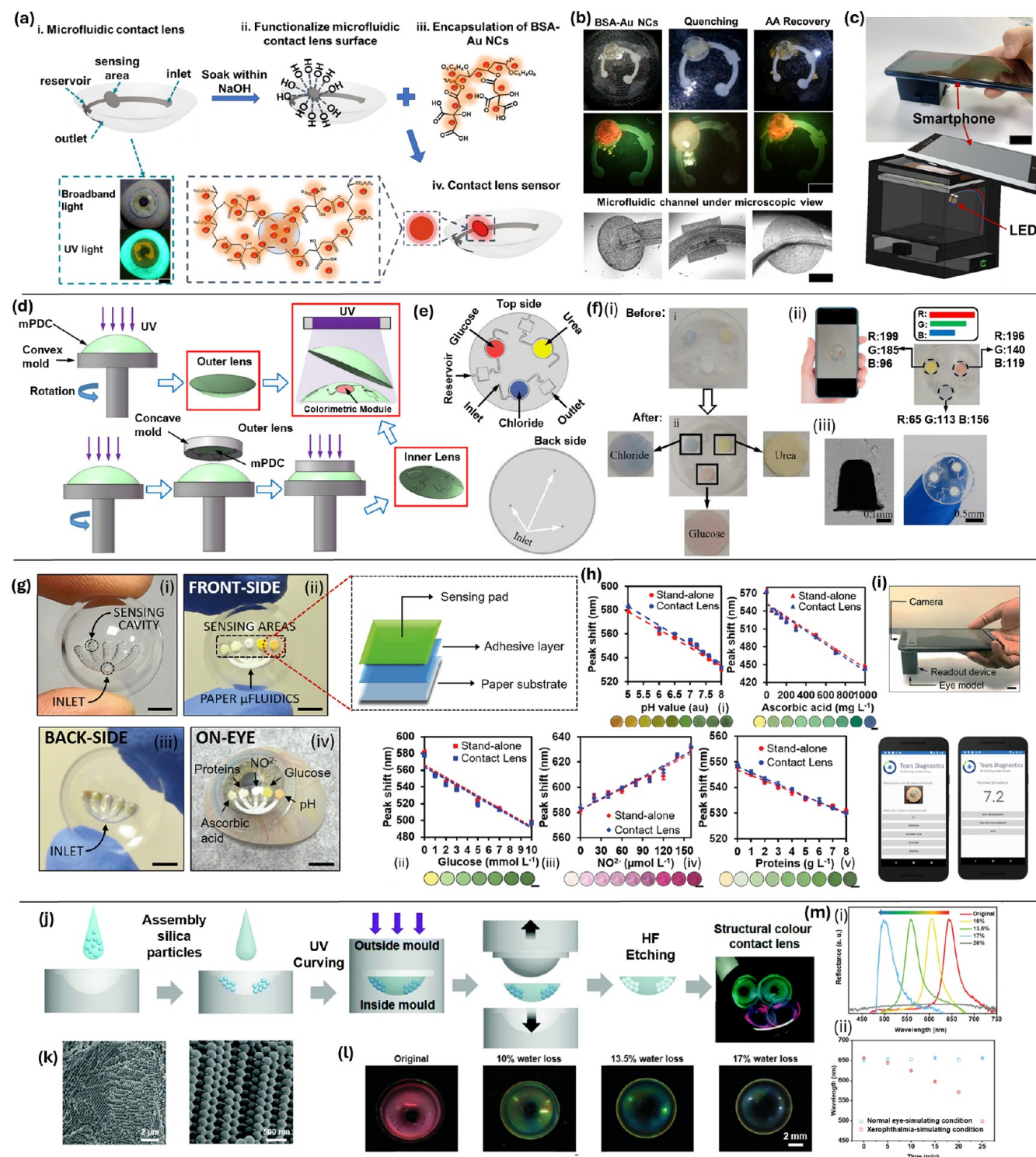


Figure 6. Fluorescent and colorimetric sensors physically embedded in contact lenses. (a) Implementation of BSA-Au NCs on microfluidic contact lenses: i. Laser-ablated microfluidic contact lens and vision site under broadband and UV light; ii. Functionalize contact lenses in 1 mol L^{-1} NaOH; iii. Encapsulate BSA-Au NCs with 15 wt % PVA and 1.5 wt % CA on the sensing region; iv Contact lens sensor for AA detection (scale bar: 2 mm). (b) Encapsulated microfluidic contact lenses and microscopic images of channels. (c) Design and photographs of the readout box for AA sensor.⁶³ Copyright 2024 Published by Elsevier B.V. (d) Fabrication process of microfluidic contact lenses. (e) Top and back sides of the inner lens. (f) i. Color change before and after tear detection; optical photos and RGB levels for glucose, chloride, and urea concentrations; ii. Procedure for harvesting tears and color analysis of digital images; iii. SEM images of the microchannel cross-section and photo of a microfluidic contact lens.¹⁰³ Copyright 2020, Springer Science Business Media (g) Device fabrication of microfluidic contact lens sensor: i. Laser-inscribed microfluidic; ii. Embedding paper microfluidic chip; iii. Backside view; iv. Contact lens on an artificial eye model (scale bars: 1.5 cm). (h) Reflection peak shift between stand-alone and contact lens-embedded sensors for i. pH sensor (range 5.0 to 8.0); ii. Ascorbic acid sensor (0 to 1.0 g L^{-1}); iii. Glucose sensor (0 to 10.0 mmol L^{-1}); iv. Nitrite sensor (0 to $160.0 \mu\text{mol L}^{-1}$); v) Protein sensor (0 to 8.0 mg mL^{-1}) (scale bar of insets: 1.5 mm). (i) Readout box for region of interest (ROI) and corresponding analyte.⁵⁰ Copyright 2020, with permission from Elsevier. (j) Structurally colored contact lens. (k) SEM images of the microchannel cross-section. (l) Contact lens on an artificial eye model. (m) Reflectance spectra and water uptake analysis.

Figure 6. continued

contact lens sensors fabrication using a colloidal crystal template of monodispersed silica particles. (l) The structurally colored lens sensor and its color change with different water loss percentages. (m) i. Reflectance spectra of the red lens sensor with varying water loss percentages. ii. Plot of wavelength changes of reflectance peaks over time under different conditions.⁷⁶ Reproduced with permission from the Royal Society of Chemistry.

highlighted through the creation of diverse holographic designs, such as rings and patches, which adapt dynamically to changes in Na^+ ion concentrations, as evidenced by their diffraction patterns. Advancing this technology, the study introduces SERS functionality to the lens surface, which is particularly notable for its glucose detection capabilities. Postnanofabrication hydrophobicity changes indicate effects on surface properties relevant to comfort and wearability.

Despite these advancements, the sensitivity of smart contact lens sensors remains insufficient for accurately detecting glucose levels within the physiological range of tear fluid. Another challenge is the nonselective binding of boronic acid derivatives to other carbohydrates and hydroxyl acids, such as lactate, which can exhibit similar concentrations to glucose, leading to potential measurement inaccuracies. To mitigate this issue, the mole fraction of 3-APB was optimized to approximately 20 mol %, significantly enhancing the sensor's selectivity for glucose and improving measurement reliability.¹⁶⁴

Physically Embedded Optical Sensors in Contact Lens. The embedding of optical sensors within contact lenses represents a classical approach in the field of ocular sensors, primarily employing fluorescence and colorimetric sensing mechanisms. In these cases, physical cavities or channels are created within the lens to accommodate various sensor elements. This fabrication method provides a protective environment for the sensors, potentially extending their operational lifespan and shielding them from direct exposure to the external environment. Embedded optical sensors facilitate multianalyte detection by integrating various sensing elements within a single lens. However, this may increase lens thickness or alter permeability, potentially affecting wearer

comfort. Balancing sensor integration with minimal lens modification remains a critical challenge in optimizing performance and user experience.

Laser-Ablated/Micro-Molded Microfluidic Channels. Microfluidic grooves carved by laser or micromold can house paper-based colorimetric strips or liquid reagents. This approach shields sensitive elements yet increases lens thickness and may reduce oxygen permeability.

An initial demonstration combined fluorescence sensing with microfluidics: bovine serum albumin–gold nanoclusters embedded in a PVA–citric acid film were cast onto a laser-ablated contact-lens substrate to monitor tear ascorbic acid (AA), a marker of ocular inflammation, in real time (Figure 6a–b).⁶³ AA restores fluorescence quenched by KMnO_4 , yielding a linear response from 0 to 1.2 mM (LOD 0.178 mM), while laser-ablated microchannels direct tear flow across the sensing film. A custom 3D-printed smartphone cradle and companion app capture and quantify emission at room temperature (Figure 6c), and the sensor maintains stable performance over 20 h of use and 10 days of storage. A simple readout box fixes the region of interest (ROI) and labels each pad by analyte to standardize on-eye imaging (Figure 6j).

Building on this microfluidic platform, a flexible, micro-molded contact lens routes tears via capillary-driven channels

from a peripheral inlet into central reservoirs preloaded with reagents for glucose, chloride, and urea (Figure 6d,e).¹⁰³ Fabricated by micro-PCR molding to define precise curvature and channel depth, the lens ensures uniform flow. Colorimetric reactions then produce hue shifts proportional to analyte concentration, which are imaged by a smartphone (Figure 6f) and analyzed via RGB-to-concentration algorithms for multiplexed tear diagnostics.

More recently, CO_2 laser ablation has been used to inscribe microchannels and biosensor-embedded microcavities directly into commercial contact lenses (Figure 6g–h). When tested with artificial tears, these devices exhibit rapid response times and high sensitivity across multiple analytes; data are processed through a smartphone-MATLAB interface (Figure 6i). Comparative measurements show consistent reflection-peak shifts for stand-alone versus lens-embedded formats across pH, ascorbic acid, glucose, nitrite, and protein.⁵⁰ Together, these approaches illustrate a progression from fluorescence to colorimetric to laser-fabricated sensing architectures, each offering unique advantages for on-eye tear analysis in both clinical and point-of-care settings.

Replica-Molded Photonic Structures. Replica molding embeds 1D/2D photonic gratings directly into the hydrogel by pressing a nanostructured master (e.g., colloidal polystyrene or silica arrays) into the prepolymer solution, UV-curing, and demolding. Within the hydrogel contact lens domain, a pHEMA lens exhibiting colorimetric responses to intraocular pressure (IOP) changes represents a significant advance.⁷⁶ The sensor is constructed by strategically assembling the hydrogel into a periodic structure using a dual-mold system followed by UV curing (Figure 6j). Unlike traditional pigmented sensors, this lens utilizes a 3D periodic structure that diffracts light based on its refractive index and the spacing of its lattice structure, causing visible color shifts correlated with IOP variations (Figure 6k).⁷⁶ SEM confirms the embedded periodicity inherited from the colloidal-crystal template, and reflectance spectra track wavelength shifts with water-loss percentages and over time. When exposed to pressures ranging from 0 to 35 kPa, the lens exhibits a pronounced blue shift across the visible spectrum, demonstrating high sensitivity and precision in pressure detection. With a detection limit within the clinically relevant range, the sensor shows potential for monitoring intraocular pressure (IOP) in conditions such as glaucoma. Its capability to detect subtle pressure variations is supported by a strong linear correlation between wavelength shifts and pressure changes, attributed to alterations in the lattice spacing of its periodic structures (Figure 6l,m).⁷⁶ This highlights its potential as a noninvasive diagnostic tool for ocular health monitoring.

Microstructural Modification of Sensors inside Contact Lens. The chemical immobilization of optical sensors in contact lenses has ushered in a new wave of sensor development. This sophisticated approach involves incorporating fluorescent dyes or other sensing probes directly into the hydrogel matrix of the lens, such as pHEMA. Unlike other methods, this technique allows for a seamless and intimate

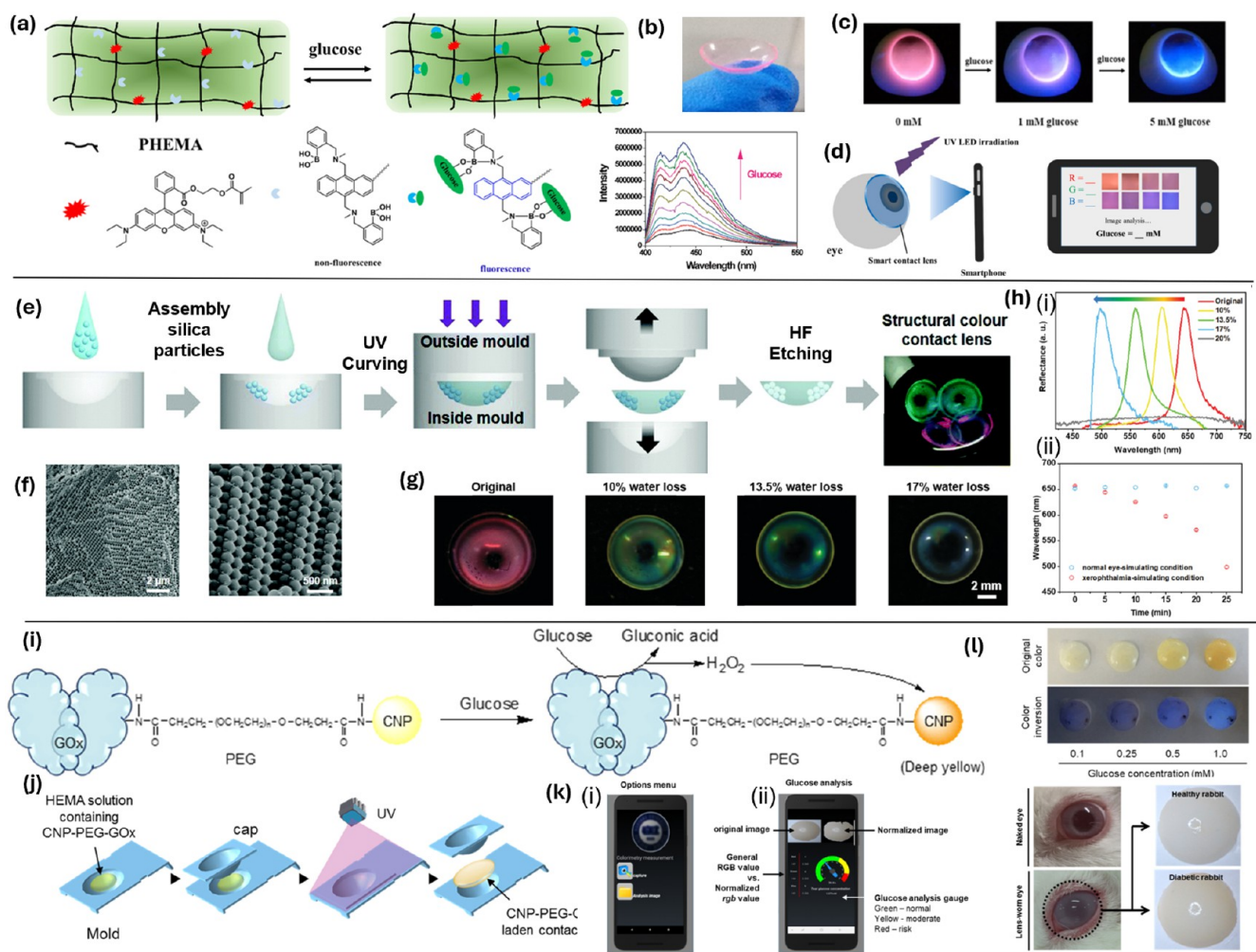


Figure 7. Chemical immobilization of optical sensors within the contact lens matrix. (a) The pHEMA hydrogel network contains a sensitive glucose probe and a calibration reference; adding glucose increases blue light emission, changing the lens fluorescence from red to blue. (b) Photograph of the soft, transparent smart contact lenses. (c) Fluorescent images of contact lenses with artificial tears at varying glucose concentrations. (d) Glucose concentration in tears is read by capturing images of the lenses on the eye and analyzing RGB values via smartphone.¹⁵⁷ Copyright 2020, with permission from Elsevier. (e) Schematics of contact lenses for single ion measurement and complete electrolyte analysis in tears. (f) Schematic of SiHG showing hydrophilic and hydrophobic interpenetrating networks; amphipathic H-ISFs are localized at the silicone-water interface; schematic cross-section of nonsilicone hydrogel lens with homogeneous structure. (g) pH-dependent equilibrium between neutral and anionic forms of 6HQ-C18, with photos of 6HQ-C18-labeled Biofinity CL at different pH under UV light. (h) Chloride quenching of SPQ-3 in water: i Emission spectra; ii Time-dependent decays ($\lambda_{ex} = 355$ nm).¹⁵⁸ Copyright 2017, with permission from Elsevier. (i) and (j) Schematics of yellow color generation by CNP-PEG-GOx and fabrication of a CNP-PEG-GOx-laden lens via photopolymerization. (k) i The interface of the glucose colorimetric detection app shows an options menu; ii The color images with RGB profiles, and calculated tear glucose concentration. (l) Relationship between lens color and complementary color at different glucose concentrations, with images of CNP-PEG-GOx-laden lenses worn by healthy or diabetic rabbits.¹⁰⁴ Copyright 2021 American Chemical Society.

interaction between the sensor and the analyte, resulting in heightened sensitivity and swift response. By manipulating the material at the molecular level, this method integrates the sensing function into the very structure of the contact lens without altering its inherent properties, such as comfort and transparency.

Physical Entrapment of Nanocluster Probes. Physical entrapment of nanoclusters leverages the hydrogel's mesh to confine particle-based probes without chemical modification. Such molecular integration is particularly advantageous for continuous monitoring and has shown promising potential in glucose detection in tear fluid. A wearable glucose-sensitive fluorescent contact lens sensor represents a breakthrough in noninvasive glucose monitoring.¹⁵⁷ By integrating a glucose-specific fluorescent probe alongside a reference dye for

calibration within a hydrogel matrix, this sensor achieves highly sensitive glucose detection directly from the contact lens environment, with the detection ranging from 0.023 to 1.0 mmol L^{-1} through an evident color shift from pink to blue (Figure 7a–c). Further underscoring its clinical viability, in vivo experiments have confirmed the biocompatibility of the sensor with the rabbit model. The sensor's detection threshold reaches $9.3 \mu\text{mol L}^{-1}$ when measured by a fluorescence spectrophotometer. This sensitivity not only enables continuous real-time monitoring of tear glucose but also distinguishes between nondiabetic and diabetic glucose levels.¹⁵⁷ A smartphone application was finally designed to facilitate the transfer and interpretation of these glucose-induced variations (Figure 7d).

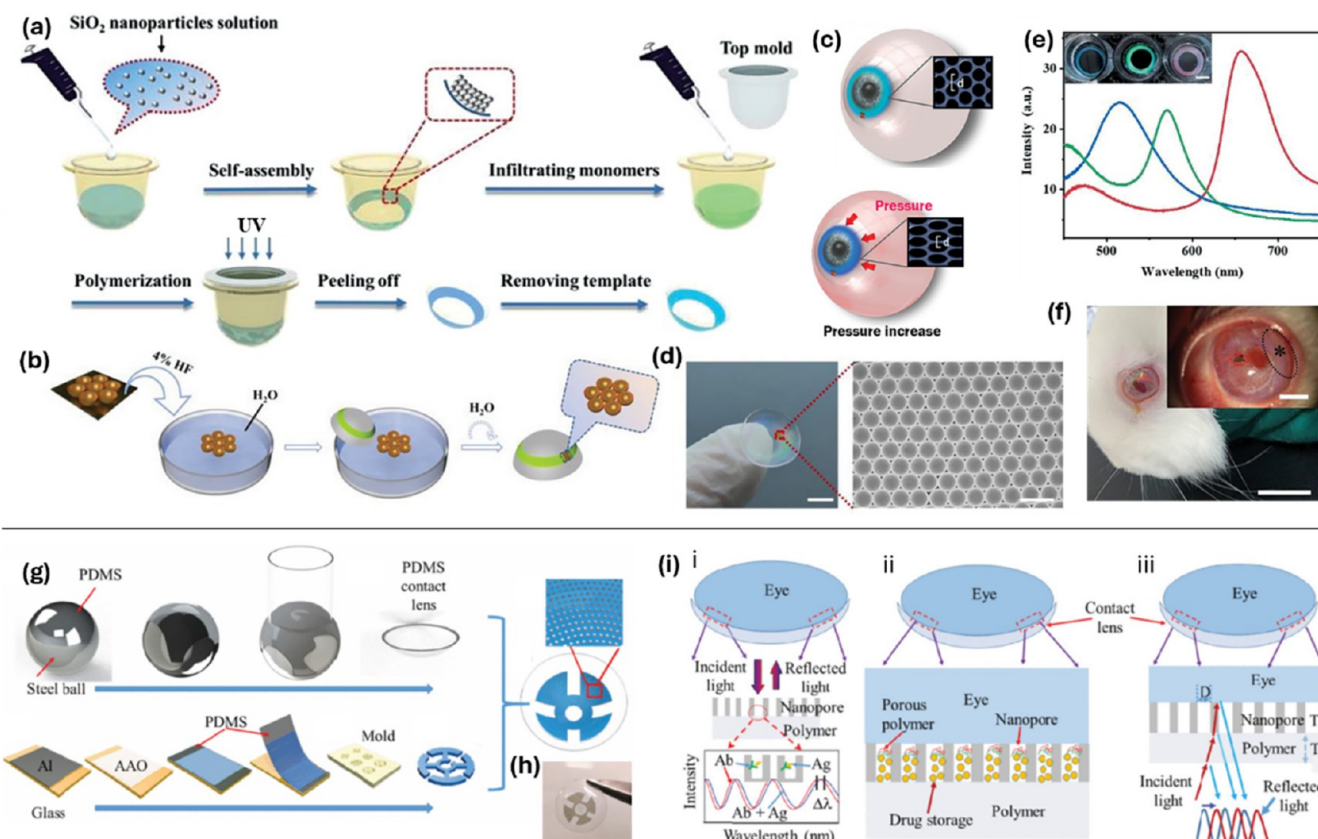


Figure 8. Multifunctional sensors across various regions of the contact lens. (a) The preparation process of structural color contact lenses involves nanoparticle self-assembly, monomer addition, polymerization, and template removal. (b) The process transfers AuNBs substrate from SiO_2/Si wafer to the contact lens. (c) Schematic of the dual-functional contact lens sensor. (d) Photograph of AuNBs substrate on the structural color contact lens and SEM image of the substrate show scale bars of 5 mm and 1 μm , respectively. (e) Reflection spectra for contact lenses displaying blue, green, and red colors, with photographs inset (scale bar: 5 mm). (f) Photograph of a rabbit wearing a smart contact lens.⁵¹ © 2022 Ye, Y. Advanced Science published by Wiley-VCH GmbH. (g) Fabrication flow of the contact lens sensor includes patterning AAO nanopore thin film sensing modules. (h) Photographs of a fabricated smart contact lens device highlight the AAO thin film's transparency in the pupil area compared to surrounding areas. (i) i Detailed view of the biomarker detection sensor where antibody–antigen binding shifts optical signal peaks. ii Details of the drug storage and release system using nanopores as containers with a porous silicone diffusion barrier for controlled release. iii Close-up of the IOP sensor showing peak shifts in the reflected optical signal corresponding to IOP changes.¹⁶⁵ Copyright 2019 IEEE.

Covalent Immobilization of Small-Molecule Fluorophores. Covalent bonding secures small-molecule fluorophores directly to the polymer backbone, preventing probe loss and ensuring stable signal output. An innovative structured silicone hydrogel (SiHG) contact lens has been advanced for precise monitoring of individual ion concentrations critical to diagnosing DED.¹⁵⁰ The architecture comprises interpenetrating hydrophilic and hydrophobic networks with amphiphatic H-ISFs localized at the silicone–water interface, contrasted with the homogeneous cross-section of a nonsilicone hydrogel lens (Figure 7e–f). These H-ISFs are integrated within the SiHG matrix, enabling real-time, noninvasive detection of key electrolytes like hydroxonium and chloride ions directly in the tear fluid. The fluorophores are covalently bonded to hydrophobic chains, ensuring their retention and functional stability within the lens structure, even under aqueous conditions.¹⁵⁰ By combining wavelength-ratiometric and lifetime-based fluorescence sensing, these lenses enable precise detection of tear composition changes critical for DED management, independent of external light conditions. This dual-sensing approach allows for the monitoring of pH-dependent transitions between neutral and anionic forms of 6HQ-C18, with fluorescence shifts visible under UV light.

Additionally, chloride ion dynamics are assessed using SPQ-3, analyzing both emission spectra and time-dependent decay rates to evaluate quenching effects (Figure 7g,h).¹⁵⁰

Enzyme–Nanoparticle Composite Embedding. Embedding enzyme–nanoparticle hybrids combines catalytic activity with nanoparticle signal enhancement in a single microdomain. Recent advancements explored the use of contact lenses for glucose detection, incorporating cerium oxide nanoparticles (CNPs) for their colorimetric response.¹⁰⁴ These CNPs are covalently linked to glucose oxidase using a biocompatible poly(ethylene glycol) linker, forming a complex that is then integrated into the (hydroxymethyl)-methacrylate (HMA) polymer network. The yellow-color generation mechanism and lens fabrication are shown schematically in Figure 7i–j. Upon exposure to glucose, this enzymatic reaction catalyzes the conversion of glucose to gluconic acid and hydrogen peroxide, the latter of which oxidizes Ce^{3+} to Ce^{4+} , resulting in a visible color change from colorless to yellow in approximately 1 min. This sensor's sensitivity exceeds 0.1 mM for glucose detection. To facilitate practical application, a smartphone-based image processing algorithm has been devised to quantify this color change with high accuracy, equating to conventional spectrophotometric methods. (Figure 7k). In vivo validation

was conducted using a transient diabetic rabbit model to assess the feasibility of CNP-PEG-GOx-laden contact lenses for tear glucose monitoring. Following glucose injection, a progressive color change was observed in the lenses, correlating with rising blood glucose levels (Figure 7i).¹⁰⁴ These findings confirm the potential of this enzyme-based contact lens sensor for noninvasive glucose monitoring in diabetes management.

Multifunctional Sensors across Various Regions of the Contact Lens. Multifunctional sensors integrated into different regions of the contact lens enable simultaneous sensing and therapeutic functions by leveraging variations in material composition or structural properties. These advanced designs allow for the concurrent detection of multiple biomarkers, environmental stimuli, or physiological changes while also serving as drug delivery platforms. Such an approach enhances the versatility of contact lens biosensors, making them highly effective for real-time, noninvasive medical diagnostics.

Structurally colored contact-lens sensors begin with the self-assembly of monodisperse SiO_2 nanoparticles into an ordered, antiopal template, which is then infiltrated with a UV-curable hydrogel precursor and selectively etched to reveal a three-dimensional photonic crystal lattice (Figure 8a,b).⁵¹ When placed on the eye, variations in intraocular pressure deform the curved antiopal structure, shifting its Bragg reflection peak across the visible spectrum (Figure 8c–e). Simultaneously, the lens surface is functionalized with peptide-modified gold nanobowls that act as SERS substrates, enabling the label-free detection of MMP-9 down to nanomolar concentrations in tear fluid. In vivo tests in rabbits over 8, 16, and 24 h show no signs of corneal irritation or damage compared to commercial lenses, confirming biocompatibility for continuous ocular monitoring (Figure 8f). Another power-free design leverages an anodic aluminum oxide (AAO) nanopore array embedded within a soft hydrogel lens to integrate three capabilities—mechanical, pharmaceutical, and biochemical—in one platform (Figure 8g–i).^{165–168} For biomarker sensing, Interleukin-12p70 antibodies immobilized in the nanopores bind antigen from tear fluid, inducing a refractive-index shift that is quantified by a compact spectrometer with pg mL^{-1} sensitivity. Concurrently, therapeutic agents loaded into the AAO pores are released steadily over 30 days directly into the tear film, providing sustained drug delivery without the need for external pumps. Ex vivo studies on cadaver pig eyes demonstrate accurate IOP measurements between 10 and 50 mmHg, attributable to curvature-dependent optical shifts of the AAO film. The unified fabrication process, based on a single photocuring step, simplifies manufacturing and ensures robust multifunctionality for POC ocular diagnostics.

CONCLUSIONS AND PERSPECTIVES

Tear fluid-based biosensing has emerged as a promising noninvasive diagnostic approach, attracting significant attention in scientific, technological, and clinical fields.^{25,26} Optical contact lens biosensors, utilizing fluorescence, colorimetry, photonics, and plasmonic sensing, have rapidly evolved, providing a highly sensitive, cost-effective platform for early disease detection. These technologies hold immense potential in monitoring ocular diseases, and systemic conditions such as diabetes, cancers, sclerosis, and neurological disorders. However, key challenges remain in improving sensor sensitivity, reproducibility, and long-term stability for clinical applications. This review explores advancements in sensing

techniques and fabrication methods, focusing on hydrogels and silicone hydrogels as primary substrate materials. Their high optical transparency, oxygen permeability, and biocompatibility make them well-suited for biosensing applications.^{52,82}

The integration of sensors into contact lenses is achieved through three main approaches: surface fabrication, microstructure embedding, and molecular modification. Surface fabrication, employing coating, grafting, or direct ablation, enables straightforward sensor attachment and rapid analyte detection but is susceptible to mechanical wear. Embedding microstructures within the lens enhances sensor protection and allows multiplexed detection but may compromise comfort and optical performance. Molecular modification integrates sensing elements within the lens matrix, improving stability and sensitivity while maintaining transparency and flexibility. Contact lens sensors are advancing toward theranostic applications, integrating biosensing and drug delivery despite challenges in fabrication and material optimization.^{165,169,170}

These advancements are expected to drive the clinical adoption of smart contact lenses, transforming wearable ocular diagnostics and treatment strategies.

Challenges and Future Perspectives. Building on recent advances in optical contact lens biosensors, key challenges and future opportunities for clinical translation must be considered from the perspectives of sensing materials, fabrication methods, biosensor integration, and real-world deployment. (i) The correlation between tear biomarkers and systemic diseases remains an area of ongoing investigation. The relatively low concentration of certain analytes in tear fluid, coupled with variations due to external factors such as hydration, diet, and circadian rhythms, presents challenges in ensuring accuracy and reliability. Large-scale clinical studies are essential to validate tear biomarkers for diagnostic applications and to establish standardized reference ranges for disease monitoring. The specificity of biosensors must also be improved to minimize interference from structurally similar molecules in tear fluid, such as lactate in glucose detection.^{171,172} (ii) The commercial viability of smart contact-lens biosensors hinges on translating lab-scale processes—molecular imprinting, nanostructured coatings, and hydrogel polymerization—into GMP/ISO 13485-compliant, high-throughput manufacturing without sacrificing sensor precision, optical clarity, or mechanical resilience over days-to-weeks of wear. Robust surface-treatment, sterilization protocols, and strict batch-to-batch consistency are essential to ensure durable performance and wearer comfort. (iii) Clinical translation and adoption will require prospective human studies that establish diagnostic accuracy, long-term ocular biocompatibility within the ISO 10993 framework, and robust performance under tear-film dynamics and real-world conditions; designs should also minimize lens-replacement frequency.^{173,174} Signals to date are mixed: the SENSIMED Triggerfish soft lens for 24 h IOP-pattern monitoring received FDA De Novo classification in 2016 (DEN140017; Class II, 21 CFR 886.1925), establishing a regulatory precedent (with special controls) for wearable ocular sensors. By contrast, the Verily/Alcon glucose-sensing lens was discontinued in 2018 after studies showed variable/lagged tear–blood correlations and susceptibility to tear-film and environmental confounders. In 2023, Mojo Vision pivoted from developing smart lenses to commercializing micro-LED displays, underscoring the engineering, power, and safety hurdles associated with continuous on-eye electronics.^{175–177} Collectively, these cases

indicate that while a pathway exists, significant validation and integration challenges remain. Going forward, developers should operate under an ISO 13485-compliant quality-management system and select the appropriate U.S. pathway—510(k), De Novo, or PMA—based on intended use and risk; in the EU, conformity with MDR 2017/745 entails notified-body oversight, UDI assignment, and EUDAMED registration.^{173,174,178,179} Reimbursement planning, user compliance (comfort and handling), and end-to-end data governance aligned to HIPAA and GDPR should be integrated from the outset through coordinated industry–clinic–academia partnerships.^{180,181} (iv) The future of smart contact lens biosensors lies in their seamless integration with wireless, self-powered, and miniaturized point-of-care (POC) devices. High-resolution smartphone imaging for real-time optical readouts, combined with cloud-based data storage and AI-driven biomarker analysis, can enhance diagnostic accuracy and enable remote patient monitoring. Emerging AI algorithms can process complex fluctuations in biomarkers, providing predictive insights for personalized medicine. Furthermore, energy-efficient power solutions, such as biofuel cells or wireless energy transfer, could enable long-term operation without external charging, improving user convenience.

With ongoing interdisciplinary efforts in materials science, bioengineering, and digital healthcare, smart contact lens biosensors hold immense potential to revolutionize patient-centric diagnostics. By overcoming current challenges and advancing toward clinical implementation, these wearable devices may pave the way for noninvasive, real-time disease monitoring, transforming the future of ophthalmology and systemic disease management.

■ AUTHOR INFORMATION

Corresponding Author

Ali K. Yetisen – Department of Chemical Engineering, Imperial College London, London SW7 2BU, U.K.;  orcid.org/0000-0003-0896-267X; Email: a.yetisen@imperial.ac.uk

Authors

Xiaoye Xia – Department of Chemical Engineering, Imperial College London, London SW7 2BU, U.K.

Yubing Hu – Department of Chemical Engineering, Imperial College London, London SW7 2BU, U.K.;  orcid.org/0000-0003-3083-0067

Nan Jiang – West China School of Basic Medical Sciences & Forensic Medicine, Sichuan University, Chengdu 610041, China; JinFeng Laboratory, Chongqing 401329, China

Complete contact information is available at:

<https://pubs.acs.org/10.1021/acssensors.Sc01222>

Notes

The authors declare no competing financial interest.

■ ACKNOWLEDGMENTS

A.K.Y. and Y.H. acknowledge the Engineering and Physical Sciences Research Council (EPSRC) (NO. EP/T013567/1). N.J. acknowledges the Fundamental Research Funds for the Central Universities (no. YJ202152), and JinFeng Laboratory, Chongqing, China (jfkjyf202203001).

■ REFERENCES

- Farandos, N. M.; Yetisen, A. K.; Monteiro, M. J.; Lowe, C. R.; Yun, S. H. Contact Lens Sensors in Ocular Diagnostics. *Adv. Healthcare Mater.* **2015**, *4* (6), 792–810.
- Juska, V. B.; Pemble, M. E. A Critical Review of Electrochemical Glucose Sensing: Evolution of Biosensor Platforms Based on Advanced Nanosystems. *Sensors* **2020**, *20* (21), No. 6013.
- Lebrecht, A.; Boehm, D.; Schmidt, M.; Koelbl, H.; Schwirz, R. L.; Grus, F. H. Diagnosis of breast cancer by tear proteomic pattern. *Cancer Genomics Proteomics* **2009**, *6* (3), 177–182.
- World Health Organization. Blindness and Visual Impairment 2023 <https://www.who.int/news-room/fact-sheets/detail/blindness-and-visual-impairment>.
- Costagliola, C.; Romano, V.; De Tullis, M.; Aceto, F.; dell’Omo, R.; Romano, M. R.; Pedicino, C.; Semeraro, F. TNF-alpha levels in tears: a novel biomarker to assess the degree of diabetic retinopathy. *Mediators Inflammation* **2013**, *2013*, No. 629529.
- Sani, E. S.; Xu, C.; Wang, C.; Song, Y.; Min, J.; Tu, J.; Solomon, S. A.; Li, J.; Banks, J. L.; Armstrong, D. G.; Gao, W. A stretchable wireless wearable bioelectronic system for multiplexed monitoring and combination treatment of infected chronic wounds. *Sci. Adv.* **2023**, *9* (12), No. eadf7388.
- Wang, M.; Yang, Y.; Min, J.; Song, Y.; Tu, J.; Mukasa, D.; Ye, C.; Xu, C.; Heflin, N.; McCune, J. S.; et al. A wearable electrochemical biosensor for the monitoring of metabolites and nutrients. *Nat. Biomed. Eng.* **2022**, *6* (11), 1225–1235.
- De la Paz, E.; Maganti, N. H.; Trifonov, A.; Jeerapan, I.; Mahato, K.; Yin, L.; Sonsa-Ard, T.; Ma, N.; Jung, W.; Burns, R.; et al. A self-powered ingestible wireless biosensing system for real-time in situ monitoring of gastrointestinal tract metabolites. *Nat. Commun.* **2022**, *13* (1), No. 7405.
- Song, J. W.; Ryu, H.; Bai, W.; Xie, Z.; Vazquez-Guardado, A.; Nandoliya, K.; Avila, R.; Lee, G.; Song, Z.; Kim, J.; et al. Biodegradable, wireless, and battery-free system for electrotherapy and impedance sensing at wound sites. *Sci. Adv.* **2023**, *9* (8), No. eade4687.
- Jiang, Y.; Trotsuk, A. A.; Niu, S.; Henn, D.; Chen, K.; Shih, C. C.; Larson, M. R.; Mermin-Bunnell, A. M.; Mittal, S.; Lai, J. C.; et al. Wireless, closed-loop, smart bandage with integrated sensors and stimulators for advanced wound care and accelerated healing. *Nat. Biotechnol.* **2023**, *41* (5), 652–662.
- An, B. W.; Shin, J. H.; Kim, S. Y.; Kim, J.; Ji, S.; Park, J.; Lee, Y.; Jang, J.; Park, Y. G.; Cho, E.; et al. Smart Sensor Systems for Wearable Electronic Devices. *Polymers* **2017**, *9* (8), No. 303.
- Kim, D.; Kim, D.; Lee, H.; Jeong, Y. R.; Lee, S. J.; Yang, G.; Kim, H.; Lee, G.; Jeon, S.; Zi, G.; et al. Body-Attachable and Stretchable Multisensors Integrated with Wirelessly Rechargeable Energy Storage Devices. *Adv. Mater.* **2016**, *28* (4), 748–756.
- Jang, K. I.; Han, S. Y.; Xu, S.; Mathewson, K. E.; Zhang, Y.; Jeong, J. W.; Kim, G. T.; Webb, R. C.; Lee, J. W.; Dawidczyk, T. J.; et al. Rugged and breathable forms of stretchable electronics with adherent composite substrates for transcutaneous monitoring. *Nat. Commun.* **2014**, *5* (1), No. 4779.
- McCall, J. G.; Kim, T. I.; Shin, G.; Huang, X.; Jung, Y. H.; Al-Hasani, R.; Omenetto, F. G.; Bruchas, M. R.; Rogers, J. A. Fabrication and application of flexible, multimodal light-emitting devices for wireless optogenetics. *Nat. Protoc.* **2013**, *8* (12), 2413–2428.
- Kim, D. H.; Lu, N.; Ma, R.; Kim, Y. S.; Kim, R. H.; Wang, S.; Wu, J.; Won, S. M.; Tao, H.; Islam, A.; et al. Epidermal electronics. *Science* **2011**, *333* (6044), 838–843.
- Shi, J.; Liu, S.; Zhang, L.; Yang, B.; Shu, L.; Yang, Y.; Ren, M.; Wang, Y.; Chen, J.; Chen, W.; et al. Smart Textile-Integrated Microelectronic Systems for Wearable Applications. *Adv. Mater.* **2020**, *32* (5), No. 1901958.
- Mukhopadhyay, S. C.; Suryadevara, N. K.; Nag, A. Wearable Sensors for Healthcare: Fabrication to Application. *Sensors* **2022**, *22* (14), No. 5137.

(18) Kaur, B.; Kumar, S.; Kaushik, B. K. Novel Wearable Optical Sensors for Vital Health Monitoring Systems-A Review. *Biosensors* **2023**, *13* (2), No. 181.

(19) Vavrinsky, E.; Esfahani, N. E.; Hausner, M.; Kuzma, A.; Rezo, V.; Donoval, M.; Kosnacova, H. The Current State of Optical Sensors in Medical Wearables. *Biosensors* **2022**, *12* (4), No. 217.

(20) Shi, Y.; Hu, Y.; Jiang, N.; Yetisen, A. K. Fluorescence Sensing Technologies for Ophthalmic Diagnosis. *ACS Sens.* **2022**, *7* (6), 1615–1633.

(21) Shi, Q.; Dong, B.; He, T.; Sun, Z.; Zhu, J.; Zhang, Z.; Lee, C. Progress in wearable electronics/photonics—Moving toward the era of artificial intelligence and internet of things. *InfoMat* **2020**, *2* (6), 1131–1162.

(22) Cho, Y. H.; Park, Y. G.; Kim, S.; Park, J. U. 3D Electrodes for Bioelectronics. *Adv. Mater.* **2021**, *33* (47), No. 2005805.

(23) Yun, S. M.; Kim, M.; Kwon, Y. W.; Kim, H.; Kim, M. J.; Park, Y.-G.; Park, J.-U. Recent Advances in Wearable Devices for Non-Invasive Sensing. *Appl. Sci.* **2021**, *11* (3), No. 1235.

(24) Kwon, Y. W.; Jun, Y. S.; Park, Y.-G.; Jang, J.; Park, J.-U. Recent advances in electronic devices for monitoring and modulation of brain. *Nano Res.* **2021**, *14* (9), 3070–3095.

(25) Yang, D. S.; Ghaffari, R.; Rogers, J. A. Sweat as a diagnostic biofluid. *Science* **2023**, *379* (6634), 760–761.

(26) Saha, T.; Songkakul, T.; Knisely, C. T.; Yokus, M. A.; Daniele, M. A.; Dickey, M. D.; Bozkurt, A.; Velev, O. D. Wireless Wearable Electrochemical Sensing Platform with Zero-Power Osmotic Sweat Extraction for Continuous Lactate Monitoring. *ACS Sens.* **2022**, *7* (7), 2037–2048.

(27) Kim, S.; Kwon, Y. W.; Seo, H.; Chung, W. G.; Kim, E.; Park, W.; Song, H.; Lee, D. H.; Lee, J.; Lee, S.; et al. Materials and Structural Designs for Neural Interfaces. *ACS Appl. Electron. Mater.* **2023**, *5* (4), 1926–1946.

(28) Oh, B.; Park, Y. G.; Jung, H.; Ji, S.; Cheong, W. H.; Cheon, J.; Lee, W.; Park, J. U. Untethered Soft Robotics with Fully Integrated Wireless Sensing and Actuating Systems for Somatosensory and Respiratory Functions. *Soft Rob.* **2020**, *7* (5), 564–573.

(29) Shi, Y.; Jiang, N.; Bikkannavar, P.; Cordeiro, M. F.; Yetisen, A. K. Ophthalmic sensing technologies for ocular disease diagnostics. *Analyst* **2021**, *146* (21), 6416–6444.

(30) Yin, X.; Zhang, S.; Lee, J. H.; Dong, H.; Mourgos, G.; Terwilliger, G.; Kraus, A.; Geraldo, L. H.; Poulet, M.; Fischer, S.; et al. Compartmentalized ocular lymphatic system mediates eye-brain immunity. *Nature* **2024**, *628* (8006), 204–211.

(31) Evans, V.; Vockler, C.; Friedlander, M.; Walsh, B.; Willcox, M. D. Lacryoglobin in human tears, a potential marker for cancer. *Clin. Exp. Ophthalmol.* **2001**, *29* (3), 161–163.

(32) Nandi, S. K.; Singh, D.; Upadhyay, J.; Gupta, N.; Dhiman, N.; Mittal, S. K.; Mahindroo, N. Identification of tear-based protein and non-protein biomarkers: Its application in diagnosis of human diseases using biosensors. *Int. J. Biol. Macromol.* **2021**, *193* (Pt A), 838–846.

(33) Keum, D. H.; Kim, S. K.; Koo, J.; Lee, G. H.; Jeon, C.; Mok, J. W.; Mun, B. H.; Lee, K. J.; Kamrani, E.; Joo, C. K.; et al. Wireless smart contact lens for diabetic diagnosis and therapy. *Sci. Adv.* **2020**, *6* (17), No. eaba3252.

(34) Li, S.; Zhu, Y.; Haghniaz, R.; Kawakita, S.; Guan, S.; Chen, J.; Li, Z.; Mandal, K.; Bahari, J.; Shah, S.; et al. A Microchambers Containing Contact Lens for the Noninvasive Detection of Tear Exosomes. *Adv. Funct. Mater.* **2022**, *32* (44), No. 2206620.

(35) Badugu, R.; Lakowicz, J. R.; Geddes, C. D. Noninvasive Continuous Monitoring of Physiological Glucose Using a Monosaccharide-Sensing Contact Lens. *Anal. Chem.* **2004**, *76* (3), 610–618.

(36) Leonardi, M.; Leuenberger, P.; Bertrand, D.; Bertsch, A.; Renaud, P. In *A Soft Contact Lens with a MEMS Strain Gage Embedded for Intraocular Pressure Monitoring*, TRANSDUCERS '03. 12th International Conference on Solid-State Sensors, Actuators and Microsystems. Digest of Technical Papers (Catal. No.03TH8664), 8–12 June 2003; IEEE, 2003; pp 1043–1046.

(37) Sen, D. K.; Sarin, G. S. Tear glucose levels in normal people and in diabetic patients. *Br. J. Ophthalmol.* **1980**, *64* (9), 693–695.

(38) Leonardi, M.; Pitchon, E. M.; Bertsch, A.; Renaud, P.; Mermoud, A. Wireless contact lens sensor for intraocular pressure monitoring: assessment on enucleated pig eyes. *Acta Ophthalmol.* **2009**, *87* (4), 433–437.

(39) Thomas, N.; Lähdesmäki, I.; Parviz, B. A. A contact lens with an integrated lactate sensor. *Sens. Actuators, B* **2012**, *162* (1), 128–134.

(40) Yao, H.; Shum, A. J.; Cowan, M.; Lähdesmäki, I.; Parviz, B. A. A contact lens with embedded sensor for monitoring tear glucose level. *Biosens. Bioelectron.* **2011**, *26* (7), 3290–3296.

(41) Chen, G.-Z.; Chan, I.-S.; Lam, D. C. Capacitive contact lens sensor for continuous non-invasive intraocular pressure monitoring. *Sens. Actuators, A* **2013**, *203*, 112–118.

(42) Choi, K.; Park, H. G. Smart Reinvention of the Contact Lens with Graphene. *ACS Nano* **2017**, *11* (6), 5223–5226.

(43) Kim, T. Y.; Mok, J. W.; Hong, S. H.; Jeong, S. H.; Choi, H.; Shin, S.; Joo, C. K.; Hahn, S. K. Wireless theranostic smart contact lens for monitoring and control of intraocular pressure in glaucoma. *Nat. Commun.* **2022**, *13* (1), No. 6801.

(44) Kim, M.; Jung, I. D.; Kim, Y.; Yun, J.; Gao, C.; Lee, H.-W.; Lee, S. W. An electrochromic alarm system for smart contact lenses. *Sens. Actuators, B* **2020**, *322*, No. 128601.

(45) Badugu, R.; Lakowicz, J. R.; Geddes, C. D. A glucose-sensing contact lens: from bench top to patient. *Curr. Opin. Biotechnol.* **2005**, *16* (1), 100–107.

(46) Ballard, Z.; Bazargan, S.; Jung, D.; Sathianathan, S.; Clemens, A.; Shir, D.; Al-Hashimi, S.; Ozcan, A. Contact lens-based lysozyme detection in tear using a mobile sensor. *Lab Chip* **2020**, *20* (8), 1493–1502.

(47) Ruan, J. L.; Chen, C.; Shen, J. H.; Zhao, X. L.; Qian, S. H.; Zhu, Z. G. A Gelated Colloidal Crystal Attached Lens for Noninvasive Continuous Monitoring of Tear Glucose. *Polymers* **2017**, *9* (4), No. 125.

(48) AlQattan, B.; Yetisen, A. K.; Butt, H. Direct Laser Writing of Nanophotonic Structures on Contact Lenses. *ACS Nano* **2018**, *12* (6), 5130–5140.

(49) Yetisen, A. K.; Jiang, N.; Gonzalez, C. M. C.; Erenoglu, Z. I.; Dong, J.; Dong, X.; Stößer, S.; Brischwein, M.; Butt, H.; Cordeiro, M. F.; et al. Scleral Lens Sensor for Ocular Electrolyte Analysis. *Adv. Mater.* **2020**, *32* (6), No. 1906762.

(50) Moreddu, R.; Wolffsohn, J. S.; Vigolo, D.; Yetisen, A. K. Laser-inscribed contact lens sensors for the detection of analytes in the tear fluid. *Sens. Actuators, B* **2020**, *317*, No. 128183.

(51) Ye, Y.; Ge, Y.; Zhang, Q.; Yuan, M.; Cai, Y.; Li, K.; Li, Y.; Xie, R.; Xu, C.; Jiang, D.; et al. Smart Contact Lens with Dual-Sensing Platform for Monitoring Intraocular Pressure and Matrix Metalloproteinase-9. *Adv. Sci.* **2022**, *9* (12), No. 2104738.

(52) Nicolson, P. C.; Vogt, J. Soft contact lens polymers: an evolution. *Biomaterials* **2001**, *22* (24), 3273–3283.

(53) Pandey, J.; Yu-Te, L.; Lingley, A.; Mirjalili, R.; Parviz, B.; Otis, B. A Fully Integrated RF-Powered Contact Lens With a Single Element Display. *IEEE Trans. Biomed. Circuits Syst.* **2010**, *4* (6), 454–461.

(54) Sun, G.; Wei, X.; Zhang, D.; Huang, L.; Liu, H.; Fang, H. Immobilization of Enzyme Electrochemical Biosensors and Their Application to Food Bioprocess Monitoring. *Biosensors* **2023**, *13* (9), No. 886.

(55) Seo, H.; Chung, W. G.; Kwon, Y. W.; Kim, S.; Hong, Y. M.; Park, W.; Kim, E.; Lee, J.; Lee, S.; Kim, M.; et al. Smart Contact Lenses as Wearable Ophthalmic Devices for Disease Monitoring and Health Management. *Chem. Rev.* **2023**, *123* (19), 11488–11558.

(56) Chu, Z.; Xue, C.; Shao, K.; Xiang, L.; Zhao, X.; Chen, C.; Pan, J.; Lin, D. Photonic crystal-embedded molecularly imprinted contact lenses for controlled drug release. *ACS Appl. Bio Mater.* **2022**, *5* (1), 243–251.

(57) Maeng, B.; Chang, H.-k.; Park, J. Photonic crystal-based smart contact lens for continuous intraocular pressure monitoring. *Lab Chip* **2020**, *20* (10), 1740–1750.

(58) Farandos, N. M.; Yetisen, A. K.; Monteiro, M. J.; Lowe, C. R.; Yun, S. H. Contact lens sensors in ocular diagnostics. *Adv. Healthcare Mater.* **2015**, *4* (6), 792–810.

(59) Elsherif, M.; Alam, F.; Salih, A. E.; AlQattan, B.; Yetisen, A. K.; Butt, H. Wearable Bifocal Contact Lens for Continual Glucose Monitoring Integrated with Smartphone Readers. *Small* **2021**, *17* (51), No. 2102876.

(60) Elsherif, M.; Hassan, M. U.; Yetisen, A. K.; Butt, H. Wearable Contact Lens Biosensors for Continuous Glucose Monitoring Using Smartphones. *ACS Nano* **2018**, *12* (6), 5452–5462.

(61) Xian, X. Frontiers of Wearable Biosensors for Human Health Monitoring. *Biosensors* **2023**, *13* (11), No. 964.

(62) Shi, Y.; Zhang, Y.; Hu, Y.; Moreddu, R.; Fan, Z.; Jiang, N.; Yetisen, A. K. Smartphone-based fluorescent sensing platforms for point-of-care ocular lactoferrin detection. *Sens. Actuators, B* **2023**, *378*, No. 133128.

(63) Shi, Y.; Wang, L.; Hu, Y.; Zhang, Y.; Le, W.; Liu, G.; Tomaschek, M.; Jiang, N.; Yetisen, A. K. Contact lens sensor for ocular inflammation monitoring. *Biosens. Bioelectron.* **2024**, *249*, No. 116003.

(64) Lin, C.; Pratt, B.; Honikel, M.; Jenish, A.; Ramesh, B.; Alkhan, A.; La Belle, J. T. Toward the Development of a Glucose Dehydrogenase-Based Saliva Glucose Sensor Without the Need for Sample Preparation. *J. Diabetes Sci. Technol.* **2018**, *12* (1), 83–89.

(65) Lim, S. H.; Martino, R.; Anikst, V.; Xu, Z.; Mix, S.; Benjamin, R.; Schub, H.; Eiden, M.; Rhodes, P. A.; Banaei, N. Rapid Diagnosis of Tuberculosis from Analysis of Urine Volatile Organic Compounds. *ACS Sens.* **2016**, *1* (7), 852–856.

(66) Farkas, Á.; Vamos, R.; Bajor, T.; Mullner, N.; Lazar, A.; Hraba, A. Utilization of lacrimal urea assay in the monitoring of hemodialysis: conditions, limitations and lacrimal arginase characterization. *Exp. Eye Res.* **2003**, *76* (2), 183–192.

(67) Berman, E. R. *Biochemistry of the Eye*; Springer Science & Business Media, 2013.

(68) Barmada, A.; Shippy, S. A. Tear analysis as the next routine body fluid test. *Eye* **2020**, *34* (10), 1731–1733.

(69) Sebbag, L.; Mochel, J. An Eye on the Dog as the Scientist's Best Friend for Translational Research in Ophthalmology: Focus on the Ocular Surface. **2020 DOI: 10.20944/preprints202005.0363.v1**.

(70) Hagan, S.; Martin, E.; Enriquez-de-Salamanca, A. Tear fluid biomarkers in ocular and systemic disease: potential use for predictive, preventive and personalised medicine. *EPMA J.* **2016**, *7* (1), No. 15.

(71) Tamhane, M.; Cabrera-Ghayouri, S.; Abelian, G.; Viswanath, V. Review of Biomarkers in Ocular Matrices: Challenges and Opportunities. *Pharm. Res.* **2019**, *36* (3), No. 40.

(72) Sen, D. K.; Sarin, G. S. Tear glucose levels in normal people and in diabetic patients. *Br. J. Ophthalmol.* **1980**, *64* (9), 693–695.

(73) Kim, J.; Kim, M.; Lee, M. S.; Kim, K.; Ji, S.; Kim, Y. T.; Park, J.; Na, K.; Bae, K. H.; Kyun Kim, H.; et al. Wearable smart sensor systems integrated on soft contact lenses for wireless ocular diagnostics. *Nat. Commun.* **2017**, *8* (1), No. 14997.

(74) Park, J.; Kim, J.; Kim, S. Y.; Cheong, W. H.; Jang, J.; Park, Y. G.; Na, K.; Kim, Y. T.; Heo, J. H.; Lee, C. Y.; et al. Soft, smart contact lenses with integrations of wireless circuits, glucose sensors, and displays. *Sci. Adv.* **2018**, *4* (1), No. eaap9841.

(75) Liu, Z.; Wang, G.; Ye, C.; Sun, H.; Pei, W.; Wei, C.; Dai, W.; Dou, Z.; Sun, Q.; Lin, C. T.; et al. An Ultrasensitive Contact Lens Sensor Based On Self-Assembly Graphene For Continuous Intraocular Pressure Monitoring. *Adv. Funct. Mater.* **2021**, *31* (29), No. 2010991.

(76) Wang, Y.; Zhao, Q.; Du, X. Structurally coloured contact lens sensor for point-of-care ophthalmic health monitoring. *J. Mater. Chem. B* **2020**, *8* (16), 3519–3526.

(77) Moreddu, R.; Wolffsohn, J. S.; Vigolo, D.; Yetisen, A. K. Laser-inscribed contact lens sensors for the detection of analytes in the tear fluid. *Sens. Actuators, B* **2020**, *317*, No. 128183.

(78) Riaz, R. S.; Elsherif, M.; Moreddu, R.; Rashid, I.; Hassan, M. U.; Yetisen, A. K.; Butt, H. Anthocyanin-Functionalized Contact Lens Sensors for Ocular pH Monitoring. *ACS Omega* **2019**, *4* (26), 21792–21798.

(79) Jiang, N.; Montelongo, Y.; Butt, H.; Yetisen, A. K. Microfluidic Contact Lenses. *Small* **2018**, *14* (15), No. 1704363.

(80) Gabriel, E. F. M.; Garcia, P. T.; Cardoso, T. M.; Lopes, F. M.; Martins, F. T.; Coltro, W. K. Highly sensitive colorimetric detection of glucose and uric acid in biological fluids using chitosan-modified paper microfluidic devices. *Analyst* **2016**, *141* (15), 4749–4756.

(81) Zhou, L.; Beuerman, R. W. Tear analysis in ocular surface diseases. *Prog. Retinal Eye Res.* **2012**, *31* (6), 527–550.

(82) Tighe, B. J. The design of polymers for contact lens applications. *Br. Polym. J.* **1976**, *8* (3), 71–77.

(83) Vincent, S. J.; Fadel, D. Optical considerations for scleral contact lenses: A review. *Contact Lens Anterior Eye* **2019**, *42* (6), 598–613.

(84) Pal, R. K.; Pradhan, S.; Narayanan, L.; Yadavalli, V. K. Micropatterned conductive polymer biosensors on flexible PDMS films. *Sens. Actuators, B* **2018**, *259*, 498–504.

(85) Ludwig, P. E.; Huff, T. J.; Zuniga, J. M. The potential role of bioengineering and three-dimensional printing in curing global corneal blindness. *J. Tissue Eng.* **2018**, *9*, No. 2041731418769863.

(86) Kihara, Si.; Yamazaki, K.; Litwak, K. N.; Litwak, P.; Kameneva, M. V.; Ushiyama, H.; Tokuno, T.; Borzelleca, D. C.; Umezawa, M.; Tomioka, J.; et al. In Vivo Evaluation of a MPC Polymer Coated Continuous Flow Left Ventricular Assist System. *Artif. Organs* **2003**, *27* (2), 188–192.

(87) Kim, S.-K.; Lee, G.-H.; Jeon, C.; Han, H. H.; Kim, S.-J.; Mok, J. W.; Joo, C.-K.; Shin, S.; Sim, J.-Y.; Myung, D.; et al. Bimetallic Nanocatalysts Immobilized in Nanoporous Hydrogels for Long-Term Robust Continuous Glucose Monitoring of Smart Contact Lens. *Adv. Mater.* **2022**, *34* (18), No. 2110536.

(88) Liu, Z.; Pflugfelder, S. C. The effects of long-term contact lens wear on corneal thickness, curvature, and surface regularity. The authors have no proprietary interest in any of the products or equipment mentioned in this article. *Ophthalmology* **2000**, *107* (1), 105–111.

(89) Lin, C.-H.; Yeh, Y.-H.; Lin, W.-C.; Yang, M.-C. Novel silicone hydrogel based on PDMS and PEGMA for contact lens application. *Colloids Surf., B* **2014**, *123*, 986–994.

(90) Musgrave, C. S. A.; Fang, F. Contact Lens Materials: A Materials Science Perspective. *Materials* **2019**, *12* (2), No. 261.

(91) Wang, J.; Fonn, D.; Simpson, T. L. Topographical thickness of the epithelium and total cornea after hydrogel and PMMA contact lens wear with eye closure. *Invest. Ophthalmol. Visual Sci.* **2003**, *44* (3), 1070–1074.

(92) Levenson, D. S. Changes in corneal curvature with long-term PMMA contact lens wear. *Eye Contact Lens* **1983**, *9* (2), 121–125.

(93) McMahon, T. T.; Zadnik, K. Twenty-five Years of Contact Lenses: The Impact on the Cornea and Ophthalmic Practice. *Cornea* **2000**, *19* (5), 730–740.

(94) Karen, K.; Yeung, O. D. a. C. S. Y. Trend-Setting: Global Lens Distribution **2011** <https://www.reviewofcontactlenses.com/article/trend-setting-global-lens-distribution>.

(95) Chen, Y.; Zhang, S.; Cui, Q.; Ni, J.; Wang, X.; Cheng, X.; Alem, H.; Tebon, P.; Xu, C.; Guo, C.; et al. Microengineered poly (HEMA) hydrogels for wearable contact lens biosensing. *Lab Chip* **2020**, *20* (22), 4205–4214.

(96) Maldonado-Codina, C.; Efron, N. Dynamic wettability of pHEMA-based hydrogel contact lenses. *Ophthalmic Physiol. Opt.* **2006**, *26* (4), 408–418.

(97) Guillou, M. Are silicone hydrogel contact lenses more comfortable than hydrogel contact lenses? *Eye Contact Lens* **2013**, *39* (1), 86–92.

(98) Stapleton, F.; Stretton, S.; Papas, E.; Skotnitsky, C.; Sweeney, D. F. Silicone hydrogel contact lenses and the ocular surface. *Ocul. Surf.* **2006**, *4* (1), 24–43.

(99) Badugu, R.; Jeng, B. H.; Reece, E. A.; Lakowicz, J. R. Contact lens to measure individual ion concentrations in tears and applications to dry eye disease. *Anal. Biochem.* **2018**, *542*, 84–94.

(100) Badugu, R.; Reece, E. A.; Lakowicz, J. R. Glucose-sensitive silicone hydrogel contact lens toward tear glucose monitoring. *J. Biomed. Opt.* **2018**, *23* (5), No. 057005.

(101) Badugu, R.; Szmacinski, H.; Reece, E. A.; Jeng, B. H.; Lakowicz, J. R. Fluorescent contact lens for continuous non-invasive measurements of sodium and chloride ion concentrations in tears. *Anal. Biochem.* **2020**, *608*, No. 113902.

(102) Moreddu, R.; Nasrollahi, V.; Kassanos, P.; Dimov, S.; Vigolo, D.; Yetisen, A. K. Lab-on-a-Contact Lens Platforms Fabricated by Multi-Axis Femtosecond Laser Ablation. *Small* **2021**, *17* (38), No. 2102008.

(103) Yang, X.; Yao, H.; Zhao, G.; Ameer, G. A.; Sun, W.; Yang, J.; Mi, S. Flexible, wearable microfluidic contact lens with capillary networks for tear diagnostics. *J. Mater. Sci.* **2020**, *55* (22), 9551–9561.

(104) Park, S.; Hwang, J.; Jeon, H.-J.; Bae, W. R.; Jeong, I.-K.; Kim, T. G.; Kang, J.; Han, Y.-G.; Chung, E.; Lee, D. Y. Cerium Oxide Nanoparticle-Containing Colorimetric Contact Lenses for Non-invasively Monitoring Human Tear Glucose. *ACS Appl. Nano Mater.* **2021**, *4* (5), 5198–5210.

(105) Badugu, R.; Lakowicz, J. R.; Geddes, C. D. Noninvasive continuous monitoring of physiological glucose using a monosaccharide-sensing contact lens. *Anal. Chem.* **2004**, *76* (3), 610–618.

(106) Moreddu, R.; Elsherif, M.; Adams, H.; Moschou, D.; Cordeiro, M. F.; Wolffsohn, J. S.; Vigolo, D.; Butt, H.; Cooper, J. M.; Yetisen, A. K. Integration of paper microfluidic sensors into contact lenses for tear fluid analysis. *Lab Chip* **2020**, *20* (21), 3970–3979.

(107) Maeng, B.; Chang, H. K.; Park, J. Photonic crystal-based smart contact lens for continuous intraocular pressure monitoring. *Lab Chip* **2020**, *20* (10), 1740–1750.

(108) Kim, M.; Choi, Y. S.; Jeong, D. H. SERS detection of dopamine using metal-chelated Ag nanoshell. *RSC Adv.* **2024**, *14* (20), 14214–14220.

(109) Tseng, R. C.; Chen, C.-C.; Hsu, S.-M.; Chuang, H.-S. Contact-Lens Biosensors. *Sensors* **2018**, *18* (8), No. 2651.

(110) Badugu, R.; Jeng, B.; Reece, E.; Lakowicz, J. Contact lens to measure individual ion concentrations in tears and applications to dry eye disease. *Anal. Biochem.* **2017**, *542*, 84–94.

(111) Thomas, N.; Lähdesmäki, I.; Parviz, B. A. A contact lens with an integrated lactate sensor. *Sens. Actuators, B* **2012**, *162*, 128–134.

(112) Wang, Z.; Dong, Y.; Sui, X.; Shao, X.; Li, K.; Zhang, H.; Xu, Z.; Zhang, D. An artificial intelligence-assisted microfluidic colorimetric wearable sensor system for monitoring of key tear biomarkers. *npj Flexible Electron.* **2024**, *8* (1), No. 35.

(113) Qin, J.; Wang, W.; Cao, L. Photonic Hydrogel Sensing System for Wearable and Noninvasive Cortisol Monitoring. *ACS Appl. Polym. Mater.* **2023**, *5* (9), 7079–7089.

(114) Qin, J.; Wang, W.; Cao, L. Photonic Hydrogel Sensing System for Wearable and Noninvasive Cortisol Monitoring. *ACS Appl. Polym. Mater.* **2023**, *5*, 7079–7089.

(115) Lakowicz, J. R.; Lakowicz, J. R. Fluorescence Sensing. In *Principles of Fluorescence Spectroscopy*; Springer, 1999; pp 531–572.

(116) Schäferling, M. The art of fluorescence imaging with chemical sensors. *Angew. Chem., Int. Ed.* **2012**, *51* (15), 3532–3554.

(117) Anzenbacher, P.; Li, F.; Palacios, M. A. Toward wearable sensors: fluorescent attoreactor mats as optically encoded cross-reactive sensor arrays. *Angew. Chem., Int. Ed.* **2012**, *51* (10), No. 2345.

(118) Yetisen, A. K.; Jiang, N.; Castaneda Gonzalez, C. M.; Erenoglu, Z. I.; Dong, J.; Dong, X.; Stosser, S.; Brischwein, M.; Butt, H.; Cordeiro, M. F.; et al. Scleral Lens Sensor for Ocular Electrolyte Analysis. *Adv. Mater.* **2020**, *32* (6), No. 1906762.

(119) Badugu, R.; Szmacinski, H.; Reece, E. A.; Jeng, B. H.; Lakowicz, J. R. Sodium-Sensitive Contact Lens for Diagnostics of Ocular Pathologies. *Sens. Actuators, B* **2021**, *331*, No. 129434.

(120) Song, Y.; Wei, W.; Qu, X. Colorimetric biosensing using smart materials. *Adv. Mater.* **2011**, *23* (37), 4215–4236.

(121) Gabriel, E. F. M.; Garcia, P. T.; Lopes, F. M.; Coltro, W. K. T. Based colorimetric biosensor for tear glucose measurements. *Micro-machines* **2017**, *8* (4), No. 104.

(122) Alexeev, V. L.; Das, S.; Finegold, D. N.; Asher, S. A. Photonic crystal glucose-sensing material for noninvasive monitoring of glucose in tear fluid. *Clin. Chem.* **2004**, *50* (12), 2353–2360.

(123) Hu, Y.; Jiang, X.; Zhang, L.; Fan, J.; Wu, W. Construction of near-infrared photonic crystal glucose-sensing materials for ratio-metric sensing of glucose in tears. *Biosens. Bioelectron.* **2013**, *48*, 94–99.

(124) Ben-Moshe, M.; Alexeev, V. L.; Asher, S. A. Fast responsive crystalline colloidal array photonic crystal glucose sensors. *Anal. Chem.* **2006**, *78* (14), 5149–5157.

(125) Ruan, J. L.; Chen, C.; Shen, J. H.; Zhao, X. L.; Qian, S. H.; Zhu, Z. G. A Gelated Colloidal Crystal Attached Lens for Noninvasive Continuous Monitoring of Tear Glucose. *Polymers* **2017**, *9* (4), No. 125.

(126) Yetisen, A. K.; Naydenova, I.; da Cruz Vasconcellos, F.; Blyth, J.; Lowe, C. R. Holographic sensors: three-dimensional analyte-sensitive nanostructures and their applications. *Chem. Rev.* **2014**, *114* (20), 10654–10696.

(127) Domschke, A.; Kabilan, S.; Anand, R.; Caines, M.; Fetter, D.; Griffith, P.; James, K.; Karangu, N.; Smith, D.; Vargas, M. et al. *Holographic Sensors in Contact Lenses for Minimally-Invasive Glucose Measurements*, Proceedings of IEEE Sensors; IEEE, 2004.

(128) Chu, Z.; Xue, C.; Shao, K.; Xiang, L.; Zhao, X.; Chen, C.; Pan, J.; Lin, D. Photonic Crystal-Embedded Molecularly Imprinted Contact Lenses for Controlled Drug Release. *ACS Appl. Bio Mater.* **2022**, *5* (1), 243–251.

(129) Elsherif, M.; Hassan, M. U.; Yetisen, A. K.; Butt, H. Glucose Sensing with Phenylboronic Acid Functionalized Hydrogel-Based Optical Diffusers. *ACS Nano* **2018**, *12* (3), 2283–2291.

(130) Kabilan, S.; Blyth, J.; Lee, M.; Marshall, A.; Hussain, A.; Yang, X. P.; Lowe, C. Glucose-sensitive holographic sensors. *J. Mol. Recognit.* **2004**, *17* (3), 162–166.

(131) Domschke, A.; March, W. F.; Kabilan, S.; Lowe, C. Initial clinical testing of a holographic non-invasive contact lens glucose sensor. *Diabetes Technol. Ther.* **2006**, *8* (1), 89–93.

(132) Liu, C.; Xu, D.; Dong, X.; Huang, Q. A review: Research progress of SERS-based sensors for agricultural applications. *Trends Food Sci. Technol.* **2022**, *128*, 90–101.

(133) Bantz, K. C.; Meyer, A. F.; Wittenberg, N. J.; Im, H.; Kurtuluş, Ö.; Lee, S. H.; Lindquist, N. C.; Oh, S.-H.; Haynes, C. L. Recent progress in SERS biosensing. *Phys. Chem. Chem. Phys.* **2011**, *13* (24), 11551–11567.

(134) Lyandres, O.; Shah, N. C.; Yonzon, C. R.; Walsh, J. T.; Glucksberg, M. R.; Van Duyne, R. P. Real-Time Glucose Sensing by Surface-Enhanced Raman Spectroscopy in Bovine Plasma Facilitated by a Mixed Decanethiol/Mercaptohexanol Partition Layer. *Anal. Chem.* **2005**, *77* (19), 6134–6139.

(135) Rycenga, M.; McLellan, J. M.; Xia, Y. A SERS study of the molecular structure of alkanethiol monolayers on Ag nanocubes in the presence of aqueous glucose. *Chem. Phys. Lett.* **2008**, *463* (1), 166–171.

(136) Mariño-López, A.; Alvarez-Puebla, R. A.; Vaz, B.; Correa-Duarte, M. A.; Perez-Lorenzo, M. SERS optical accumulators as unified nanoplatforms for tear sampling and sensing in soft contact lenses. *Nanoscale* **2022**, *14* (22), 7991–7999.

(137) Zhang, Y.-J.; Ze, H.; Fang, P.-P.; Huang, Y.-F.; Kudelski, A.; Fernández-Vidal, J.; Hardwick, L. J.; Lipkowski, J.; Tian, Z.-Q.; Li, J.-F. Shell-isolated nanoparticle-enhanced Raman spectroscopy. *Nat. Rev. Methods Primers* **2023**, *3* (1), No. 36.

(138) Ding, S.-Y.; Yi, J.; Li, J.-F.; Ren, B.; Wu, D.-Y.; Panneerselvam, R.; Tian, Z.-Q. Nanostructure-based plasmon-enhanced Raman spectroscopy for surface analysis of materials. *Nat. Rev. Mater.* **2016**, *1* (6), No. 16021.

(139) Jiang, S.; Cao, Z. Ultralow-Fouling, Functionalizable, and Hydrolyzable Zwitterionic Materials and Their Derivatives for Biological Applications. *Adv. Mater.* **2010**, *22* (9), 920–932.

(140) Tighe, B. J. A Decade of Silicone Hydrogel Development: Surface Properties, Mechanical Properties, and Ocular Compatibility. *Eye Contact Lens* **2013**, *39* (1), 4–12.

(141) Love, J. C.; Estroff, L. A.; Kriebel, J. K.; Nuzzo, R. G.; Whitesides, G. M. Self-Assembled Monolayers of Thiolates on Metals as a Form of Nanotechnology. *Chem. Rev.* **2005**, *105* (4), 1103–1170.

(142) Peppas, N. A.; Bures, P.; Leobandung, W.; Ichikawa, H. Hydrogels in pharmaceutical formulations. *Eur. J. Pharm. Biopharm.* **2000**, *50* (1), 27–46.

(143) Shi, Y.; Wang, L.; Hu, Y.; Zhang, Y.; Le, W.; Liu, G.; Tomaschek, M.; Jiang, N.; Yetisen, A. K. Contact lens sensor for ocular inflammation monitoring. *Biosens. Bioelectron.* **2024**, *249*, No. 116003.

(144) Isgor, P. K.; Abbasiasl, T.; Das, R.; Istif, E.; Yener, U. C.; Beker, L. Paper integrated microfluidic contact lens for colorimetric glucose detection. *Sens. Diagn.* **2024**, *3* (10), 1743–1748.

(145) Vural, B.; Uludağ, İ.; Ince, B.; Özeturk, C.; Özeturk, F.; Sezgintürk, M. K. Fluid-based wearable sensors: a turning point in personalized healthcare. *Turk. J. Chem.* **2023**, *47* (5), 944–967.

(146) Elsherif, M.; Moreddu, R.; Alam, F.; Salih, A. E.; Ahmed, I.; Butt, H. Wearable Smart Contact Lenses for Continual Glucose Monitoring: A Review. *Front. Med.* **2022**, *9*, No. 858784.

(147) Chen, C.; Dong, Z.-Q.; Shen, J.-H.; Chen, H.-W.; Zhu, Y.-H.; Zhu, Z.-G. 2D Photonic Crystal Hydrogel Sensor for Tear Glucose Monitoring. *ACS Omega* **2018**, *3* (3), 3211–3217.

(148) Park, Y.; Kim, U. J.; Lee, S.; Kim, H.; Kim, J.; Ma, H.; Son, H.; Yoon, Y. Z.; Lee, J.-s.; Park, M.; et al. On-chip Raman spectrometers using narrow band filter array combined with CMOS image sensors. *Sens. Actuators, B* **2023**, *381*, No. 133442.

(149) Kerman, S.; Luo, X.; Ding, Z.; Zhang, Z.; Deng, Z.; Qin, X.; Xu, Y.; Zhai, S.; Chen, C. Scalable miniature on-chip Fourier transform spectrometer for Raman spectroscopy. *Light: Sci. Appl.* **2025**, *14* (1), No. 208.

(150) Badugu, R.; Jeng, B. H.; Reece, E. A.; Lakowicz, J. R. Contact lens to measure Individual ion concentrations in tears and applications to dry eye disease. *Anal. Biochem.* **2018**, *542*, 84–94.

(151) Jiang, N.; Montelongo, Y.; Butt, H.; Yetisen, A. K. Microfluidic Contact Lenses. *Small* **2018**, *14* (15), No. 1704363.

(152) M, A.; Saxena, A.; Mishra, D.; Singh, K.; George, S. D. Microfluidic contact lens: fabrication approaches and applications. *Microsyst. Nanoeng.* **2025**, *11* (1), No. 59.

(153) Yang, X.; Pan, X.; Blyth, J.; Lowe, C. R. Towards the real-time monitoring of glucose in tear fluid: holographic glucose sensors with reduced interference from lactate and pH. *Biosens. Bioelectron.* **2008**, *23* (6), 899–905.

(154) Lee, W.-C.; Koh, E. H.; Kim, D.-H.; Park, S.-G.; Jung, H. S. Plasmonic contact lens materials for glucose sensing in human tears. *Sens. Actuators, B* **2021**, *344*, No. 130297.

(155) March, W. F.; Mueller, A.; Herbrechtsmeier, P. Clinical trial of a noninvasive contact lens glucose sensor. *Diabetes Technol. Ther.* **2004**, *6* (6), 782–789.

(156) March, W.; Lazzaro, D.; Rastogi, S. Fluorescent measurement in the non-invasive contact lens glucose sensor. *Diabetes Technol. Ther.* **2006**, *8* (3), 312–317.

(157) Deng, M.; Song, G.; Zhong, K.; Wang, Z.; Xia, X.; Tian, Y. Wearable fluorescent contact lenses for monitoring glucose via a smartphone. *Sens. Actuators, B* **2022**, *352*, No. 131067.

(158) Jeon, H. J.; Kim, S.; Park, S.; Jeong, I. K.; Kang, J.; Kim, Y. R.; Lee, D. Y.; Chung, E. Optical Assessment of Tear Glucose by Smart Biosensor Based on Nanoparticle Embedded Contact Lens. *Nano Lett.* **2021**, *21* (20), 8933–8940.

(159) Moreddu, R.; Elsherif, M.; Butt, H.; Vigolo, D.; Yetisen, A. K. Contact lenses for continuous corneal temperature monitoring. *RSC Adv.* **2019**, *9* (20), 11433–11442.

(160) Salih, A. E.; Butt, H. Multifunctional transition and temperature-responsive contact lenses. *Light: Sci. Appl.* **2023**, *12* (1), No. 271.

(161) Deng, J.; Chen, S.; Chen, J.; Ding, H.; Deng, D.; Xie, Z. Self-Reporting Colorimetric Analysis of Drug Release by Molecular Imprinted Structural Color Contact Lens. *ACS Appl. Mater. Interfaces* **2018**, *10* (40), 34611–34617.

(162) Lee, W.-C.; Koh, E. H.; Kim, D.-H.; Park, S.-G.; Jung, H. S. Plasmonic contact lens materials for glucose sensing in human tears. *Sens. Actuators, B* **2021**, *344*, No. 130297.

(163) Narasimhan, V.; Siddique, R. H.; Kim, U. J.; Lee, S.; Kim, H.; Roh, Y.; Wang, Y. M.; Choo, H. Glasswing-Butterfly-Inspired Multifunctional Scleral Lens and Smartphone Raman Spectrometer for Point-of-Care Tear Biomarker Analysis. *Adv. Sci.* **2023**, *10* (5), No. 2205113.

(164) Kabilan, S.; Marshall, A. J.; Sartain, F. K.; Lee, M. C.; Hussain, A.; Yang, X.; Blyth, J.; Karangu, N.; James, K.; Zeng, J.; et al. Holographic glucose sensors. *Biosens. Bioelectron.* **2005**, *20* (8), 1602–1610.

(165) Song, C.; Ben-Shlomo, G.; Que, L. A Multifunctional Smart Soft Contact Lens Device Enabled by Nanopore Thin Film for Glaucoma Diagnostics and In Situ Drug Delivery. *J. Microelectromech. Syst.* **2019**, *28* (5), 810–816.

(166) Alzghoul, S.; Hailat, M.; Zivanovic, S.; Que, L.; Shah, G. V. Measurement of serum prostate cancer markers using a nanopore thin film based optofluidic chip. *Biosens. Bioelectron.* **2016**, *77*, 491–498.

(167) Feng, S.; Chen, C.; Wang, W.; Que, L. An aptamer nanopore-enabled microsensor for detection of theophylline. *Biosens. Bioelectron.* **2018**, *105*, 36–41.

(168) Song, C.; Deng, P.; Que, L. Rapid multiplexed detection of beta-amyloid and total-tau as biomarkers for Alzheimer's disease in cerebrospinal fluid. *Nanomedicine* **2018**, *14* (6), 1845–1852.

(169) Yang, C.; Wu, Q.; Liu, J.; Mo, J.; Li, X.; Yang, C.; Liu, Z.; Yang, J.; Jiang, L.; Chen, W.; et al. Intelligent wireless theranostic contact lens for electrical sensing and regulation of intraocular pressure. *Nat. Commun.* **2022**, *13* (1), No. 2556.

(170) Ma, X.; Ahadian, S.; Liu, S.; Zhang, J.; Liu, S.; Cao, T.; Lin, W.; Wu, D.; de Barros, N. R.; Zare, M. R.; et al. Smart Contact Lenses for Biosensing Applications. *Adv. Intell. Syst.* **2021**, *3* (5), No. 2000263.

(171) Freeman, D. M. E.; Ming, D. K.; Wilson, R.; Herzog, P. L.; Schulz, C.; Felice, A. K. G.; Chen, Y. C.; O'Hare, D.; Holmes, A. H.; Cass, A. E. G. Continuous Measurement of Lactate Concentration in Human Subjects through Direct Electron Transfer from Enzymes to Microneedle Electrodes. *ACS Sens.* **2023**, *8* (4), 1639–1647.

(172) Wu, W.; Wang, L.; Yang, Y.; Du, W.; Ji, W.; Fang, Z.; Hou, X.; Wu, Q.; Zhang, C.; Li, L. Optical flexible biosensors: From detection principles to biomedical applications. *Biosens. Bioelectron.* **2022**, *210*, No. 114328.

(173) *10993–1:2018 Biological Evaluation of Medical Devices – Part 1: Evaluation and Testing within a Risk Management Process*; ISO, 2018.

(174) U.S. Food and Drug Administration. De Novo Classification Request for SENSIMED Triggerfish 2016 https://www.accessdata.fda.gov/cdrh_docs/reviews/DEN140017.pdf (accessed August 25, 2025).

(175) STAT. Verily and Alcon Halt Glucose-Sensing Contact Lens Project 2018 <https://www.statnews.com/2018/11/16/verily-alcon-halt-glucose-sensing-contact-lens/> (accessed August 25, 2025).

(176) Mojo Vision. Mojo Vision Pivots to Micro-LED Display Commercialization 2023 <https://www.mojo.vision/news/mojo-vision-pivots-microled> (accessed August 25, 2025).

(177) U.S. Food and Drug Administration (FDA). e Novo Classification Request for SENSIMED TRIGGERFISH (DEN140017) 2016 <https://www.accessdata.fda.gov/scripts/cdrh/cfdocs/cfpmn/denovo.cfm?id=DEN140017> (accessed August 29, 2025).

(178) EUR-Lex. Regulation (EU) 2017/745 of the European Parliament and of the Council on Medical Devices (Consolidated Text) 2021 <https://eur-lex.europa.eu/eli/reg/2017/745/oj> (accessed August 12, 2025).

(179) European Commission. European Database on Medical Devices (EUDAMED) 2025 <https://health.ec.europa.eu/system/>

files/2023-01/md_eudamed_overview_en.pdf (accessed August 11, 2025).

(180) U.S. Department of Health and Human Services. Summary of the HIPAA Privacy Rule 2023 <https://www.hhs.gov/hipaa/for-professionals/privacy/laws-regulations/index.html> (accessed August 22, 2025).

(181) European Commission. EU Data Protection Rules (GDPR) 2025 https://commission.europa.eu/law/law-topic/data-protection/eu-data-protection-rules_en (accessed August 21, 2025).